X.1

Late Variscan Deformation in the Iberian Peninsula; a Late Feature in the Laurentia-Gondwana Dextral Collision

Index

X.1.1. Introduction

A complex network of major shear zones was developed during the last stages of intracontinental deformation of the Variscan orogeny. This Late Variscan deformation episode was considered the result of internal deformation along first order E-W dextral shear zones (Arthaud and Matte, 1975; 1977). Such kinematics is often considered a pervasive feature of most of the Variscan orogenic evolution (Ribeiro *et al.*, 1995; Shelley and Bossière, 2000; 2002;

Ribeiro, 2002; Ribeiro *et al.*, 2007; Martínez Catalán, 2011; Nance *et al.*, 2012; Dias *et al.*, 2016). In the Iberian Massif this Late Variscan deformation gave rise to some of the most important observed basement faults (Ribeiro, 1974; Iglesias and Ribeiro, 1981), like the NNE-SSW Vilariça and Régua-Chaves-Verin faults in NW Iberia (Ribeiro *et al.*, 1990; Marques *et al.*, 2002; Dias *et al.*, 2013). Although several works focus on this major event there are still some doubts concerning the kinematics and the timing of the deformation. Such controversy mainly results from the strong reworking of the Late Variscan structures by the Meso-Cenozoic deformation episodes. The scarcity of Lower Mesozoic outcrops in the vicinity of these major structures strongly limits the temporal constrain of observed deformations to the Palaeozoic. The transition between the Late Variscan wrench faulting and the early Alpine extensional regime is essential to the understanding of the Late Palaeozoic dynamics of Western Europe. In such a debate, the Variscan kinematics of the NNE-SSW main faults is crucial because they have been considered, either sinistral (Ribeiro, 1974; Ribeiro *et al.*, 2007; Moreira *et al.*, 2010; 2014; Dias and Basile, 2013), or dextral with a sinistral kinematics alpine reworking (Marques *et al.*, 2002). Obviously such opposite interpretations give rise to strongly different geodynamical models for the transition between the late stages of the collision that formed the Pangaea, and the beginning of its dispersion leading to the opening of the Atlantic Ocean.

The SW Portuguese coast, where the outcrops are remarkably well exposed, is a key sector to discriminate between the previous models. Indeed, in this region it is possible to highlight:

- A continuity between the sedimentation of the Upper Carboniferous turbiditic sediments (Moscovian; Pereira *et al.*, 2007) and the late stages of the Variscan deformation (Dias and Basile, 2013);
- The influence of the brittle-ductile Late Variscan structures in the opening of the intracontinental Triassic rift basins (Dias and Ribeiro, 2002; Dias and Basile, 2013).

In this paper, new detailed structural mapping in two key sectors of SW Portugal enables the understanding of the kinematical, chronological and geodynamical behaviour of the Late Variscan deformation in Iberia.

X.1.2. Geological Setting of Southwest Iberian Variscides

The main Variscan structure in the South Portuguese Zone is a typical fold and thrust belt (Ribeiro *et al.*, 1979, 1983; Ribeiro and Silva, 1983; Silva *et al.*, 1990) with a slightly arcuate pattern ranging from NW-SE to a NNW-SSE trend towards W (Fig. 1A; *e.g.* Ribeiro *et al.*, 1979; Dias and Basile, 2013). This deformation was the result of the basin inversion induced by the

SW Iberia Variscan subduction zone (Ribeiro *et al.*, 2007). Such process generated a SW facing imbricated complex (Fig. 1B), related to a thin skinned tectonic regime (Ribeiro and Silva, 1983; Ribeiro *et al.*, 1983).

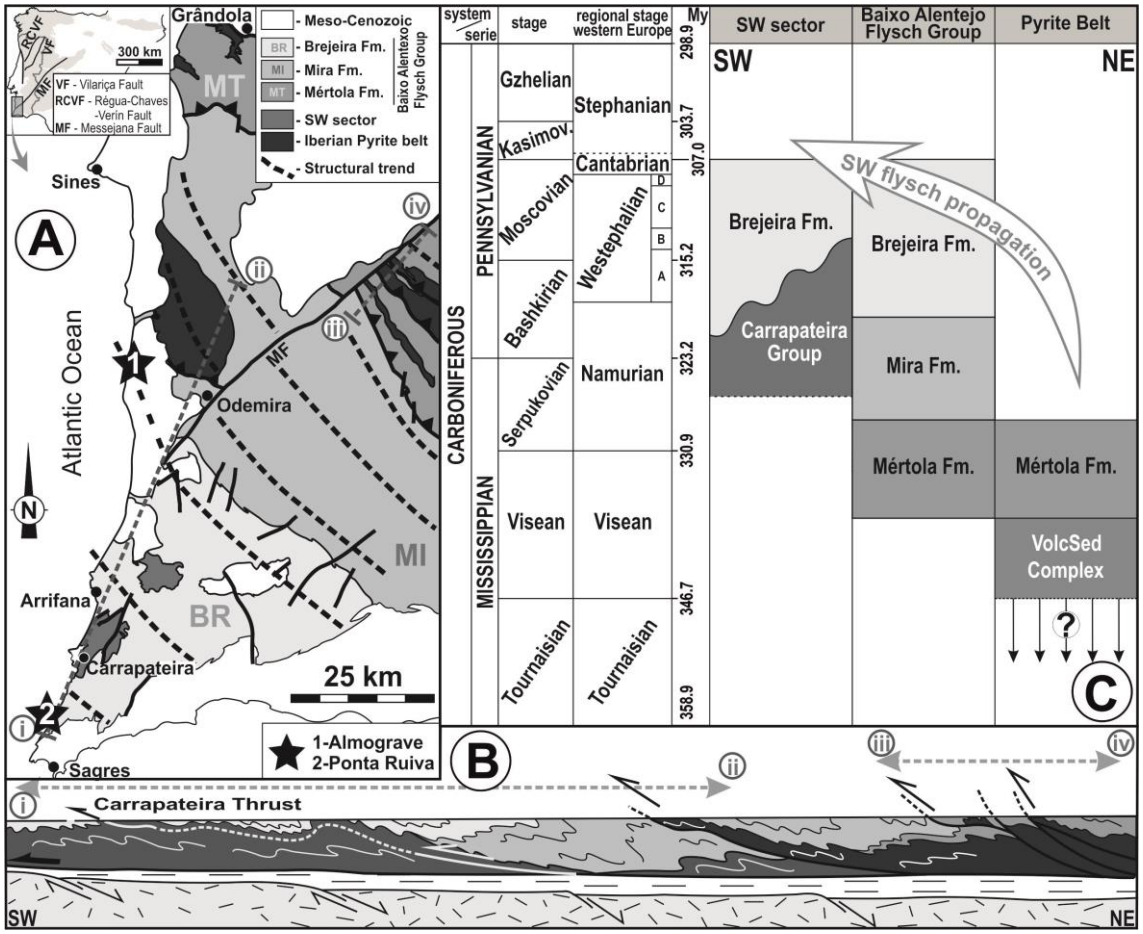

Figure 1 – Main geological features of the southern Portuguese Variscides.

A – Spatial distribution of the main geological domains (adapted from Oliveira, 1984; Ribeiro *et al.*, 1979).

B – Geological profile along the South-Portuguese zone (adapted from Ribeiro *et al.*, 2007; location is shown in figure 1A).

C – Main lithostratigraphic units emphasizing the Carboniferous turbidites (adapted from Oliveira, 1990; Silva *et al.*, 1990; 2113; Oliveira *et al.*, 2013).

The lithostratigraphy of the South Portuguese Zone allows the individualization of three domains in SW Portugal (see Oliveira *et al.*, 2013 for a review); from NE to SW, the Pyrite Belt, Baixo Alentejo Flysch Group and Southwest Sector (Fig. 1C). In the framework of this work the Baixo Alentejo Flysch Group, a deep water turbidite sequence with more than 5 km thickness (Oliveira *et al.*, 2013) must be highlighted. Sedimentological and paleontological data allow the

establishment of three main lithostratigraphic units in this group (Oliveira, 1990): Mértola, Mira and Brejeira formations. The spatial relation of these units shows a southward propagating of the basin, from Upper Visean to Upper Moscovian (Oliveira *et al.*, 2013; Jorge *et al.*, 2013).

The continuous interaction between deformation and sedimentation (Ribeiro and Silva, 1983) highlights a diachronous propagation of the deformation from NE to SW in a piggy back regime (Carvalho *et al.*, 1971; Silva, 1989; Silva *et al.*, 1990). The deeper structural levels with a pervasive cleavage are thus present in the NE, while southwards a shallower deformation is found (Ribeiro *et al.*, 1983; Marques *et al.*, 2010; Dias and Basile, 2013). The Variscan metamorphic grade reflects the structural pattern, ranging from the greenschist facies in the NE to top diagenesis / anchizone toward the SW (Schermerhorn, 1971; Munhá, 1983; Abad *et al.*, 2004).

Although strongly deformed, the general pattern of the SW Variscan imbricated complex is the result of a very homogeneous stress field. This lead to consider an unique and continuous diachronous tectonic phase (Ribeiro *et al.*, 1979; Ribeiro and Silva, 1983; Caroça and Dias, 2001; Marques *et al.*, 2010; Reber *et al.*, 2010; Zulauf *et al*, 2011; Dias and Basile, 2013). As it is the first and main tectonic phase found in this sector, it is usually considered a local D_1 event (Ribeiro, 1983; Ribeiro and Silva, 1983; Silva *et al.*, 1990; Dias and Caroça, 2001; Marques *et al.*, 2010; Dias and Basile, 2013).

The understanding of the D_1 structures in the external sectors of SW Iberia is essential to the study of the more discrete and heterogeneous Late Variscan deformation (D_2) which developed in a different geodynamical context (Dias and Basile, 2013).

X.1.3. The First Variscan Deformation Phase (D_1) in SW of South Portuguese Zone

The D_1 structures overlap syn-sedimentary normal faults with local expression. Although they have been considered the result of an extensional regional environment leading to the deepening of the sedimentary basins (Marques *et al.*, 2010), they could also result from flexural extension, due to bending of lithospheric plate, in the foredeep-foreland transition zones during collisional processes (*e.g.* Bradley and Kidd, 1991; Scisciani *et al.*, 2001).

The continuity of the shortening related to the D_1 tectonic event gives rise to a frequent superposition of mesoscopic structures with complex interference patterns. As these structures share a common stress field, they must be ascribed to the same deformation phase. Nevertheless, their well defined geometry and kinematics made possible the subdivision of several stages.

The oldest D_1 structures (D_{1a}) were developed by layer parallel shortening (Fig. 2A), when the layers were still sub-horizontal. In the more competent quartzwacke layers conjugated shear zones underlined by en-echelon quartz veins were developed (Marques *et al*., 2010; Dias and Basile, 2013). The trends of the conjugate dextral NNE-SSW and the sinistral ENE-WSW to E-W shear zones indicate a stress field with a sub-horizontal NE-SW σ_1, a NW-SE σ_3 also sub-horizontal and a sub-vertical σ_2. Quartzwacke boudins and extensional fractures orthogonal to σ_3 are common structures. In the pelitic layers this early tectonic shortening was accommodated essentially by thickening.

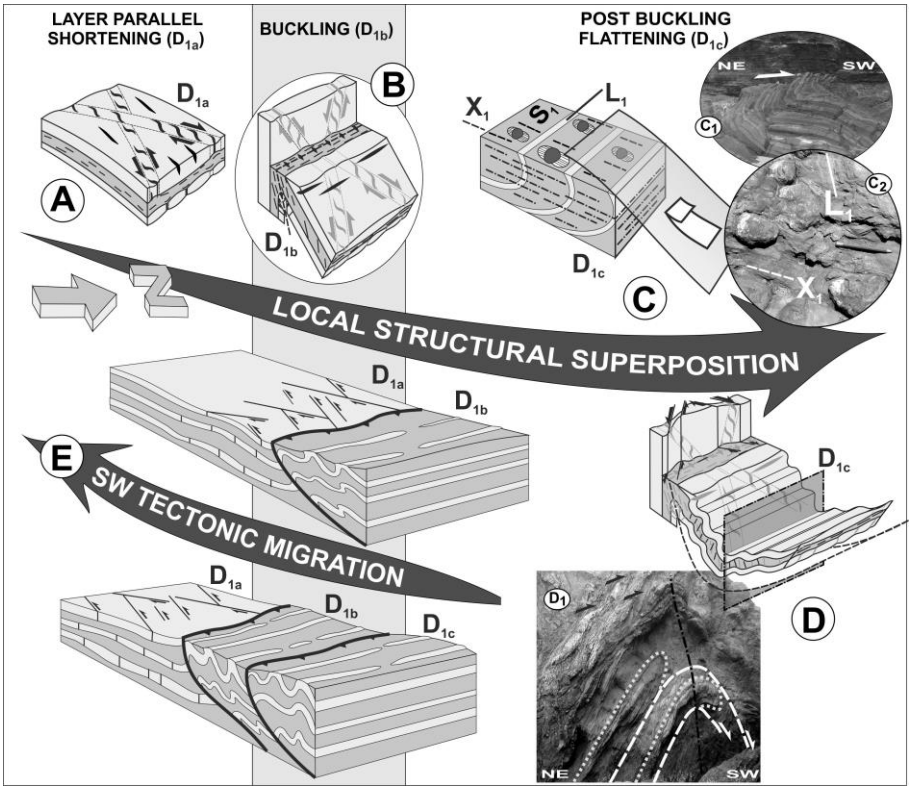

Figure 2 – Main structural features of the D_1 deformation evolution in SW Portugal (adapted from Dias and Basile, 2013).

A – Conjugated shear zones and extensional fractures developed during D_{1a} layer parallel shortening stage;

B – D_{1b} folds with outer arc extensional veins (in black) cutting D_{1a} en echelon quartz veins (in gray);

C – D_{1c} thrusts cutting previous folds (C_1- Mouranitos thrust north of Sagres) emphasizing the X_1 stretching lineation orthogonal to fold axes (C_2- quartz pressure shadows parallel to stretching lineation in Carrapateira nappe);

D – D_{1c} deformation superposed on previous D_1 folds and thrusts (D_1 in the Sagres sector);

E – Diachronous D_1 SW migration.

The continuity of the compressive deformation induced general folding (D_{1b}), not only of the layers, but also of the D_{1a} structures (Fig. 2B). As expected in a SW propagating fold and thrust belt (Carvalho *et al.*, 1971), the vergence of these folds is towards the SW foreland. As the folds have been developed in a relatively upper structural level (Marques *et al.*, 2010; Zulauf *et al.,* 2011) the axial planar S_1 cleavage is only predominant in the hinge zones and reverse limbs of the D_{1b} folds, affecting preferentially the more pelitic lithologies.

Probably related with the post buckling flattening (Marques *et al.*, 2010), low dipping thrusts where formed (Fig. 2C; Ribeiro, 1983; Ribeiro *et al.*, 1983; Caroça and Dias, 2001; Dias and Basile, 2013). Due to the out of sequence propagation of these thrusts (Ribeiro, 1983; Ribeiro and Silva, 1983), which are considered D_{1c} structures, they often cut previous D_{1b} folds (Fig. $2C_1$). In the vicinity of major thrusts (*e.g.* the Carrapateira nappe; Ribeiro, 1983; Fig. 1B), a stretching lineation (X_{1c}) is found parallel to the top-to-SW Variscan transport. This lineation is parallel to quartz fibres in pressure shadows adjacent to pyrite crystals (Fig. $2C_2$).

The effect of this post buckling D_{1c} shortening on previous folds is mostly controlled by the D_{1b} geometry (Fig. 2D). In the steeply dipping short limbs, the late regional D_1 shortening produced conjugated brittle to brittle-ductile subvertical D_{1c} shear zones: N-S to NNE-SSW dextral and ENE-WSW to E-W sinistral (Caroça and Dias, 2001; Marques *et al.*, 2010). In the low dipping D_{1b} normal limbs and early D_{1c} thrusts, the late shortening mostly induced the formation of open to tight folds with sub-vertical axial planes and sub-horizontal fold hinges, which refolded the older structures (Fig. $2D_1$; Caroça and Dias, 2001).

Although the use of previous D_1 deformation stages is useful at local scale, care should be taken at the regional level due to the diachronous propagation of the deformation (Fig. 2E).

X.1.4. Variscan Geometry and Kinematics at external domains of the South Portuguese Zone

In order to improve the knowledge of the Late Variscan deformation in SW Iberia two sectors have been chosen: Almograve and Ponta Ruiva (Fig. 1A). While in Almograve it is possible to detail the superposition of different stages related to the Variscan deformation, in Ponta Ruiva their relation with the extensional Triassic events, due to the opening of the Atlantic Ocean, can also be studied.

X.1.4.1. The Almograve Sector

The most evident structures in Almograve are the sudden regional D_1 strike changes by decametric to hectometric NNE-SSW brittle to brittle-ductile kink-bands (Fig. 3). Although well

exposed, its genesis is debatable (Caroça and Dias, 2002; Marques *et al.*, 2010; Dias and Basile, 2013).

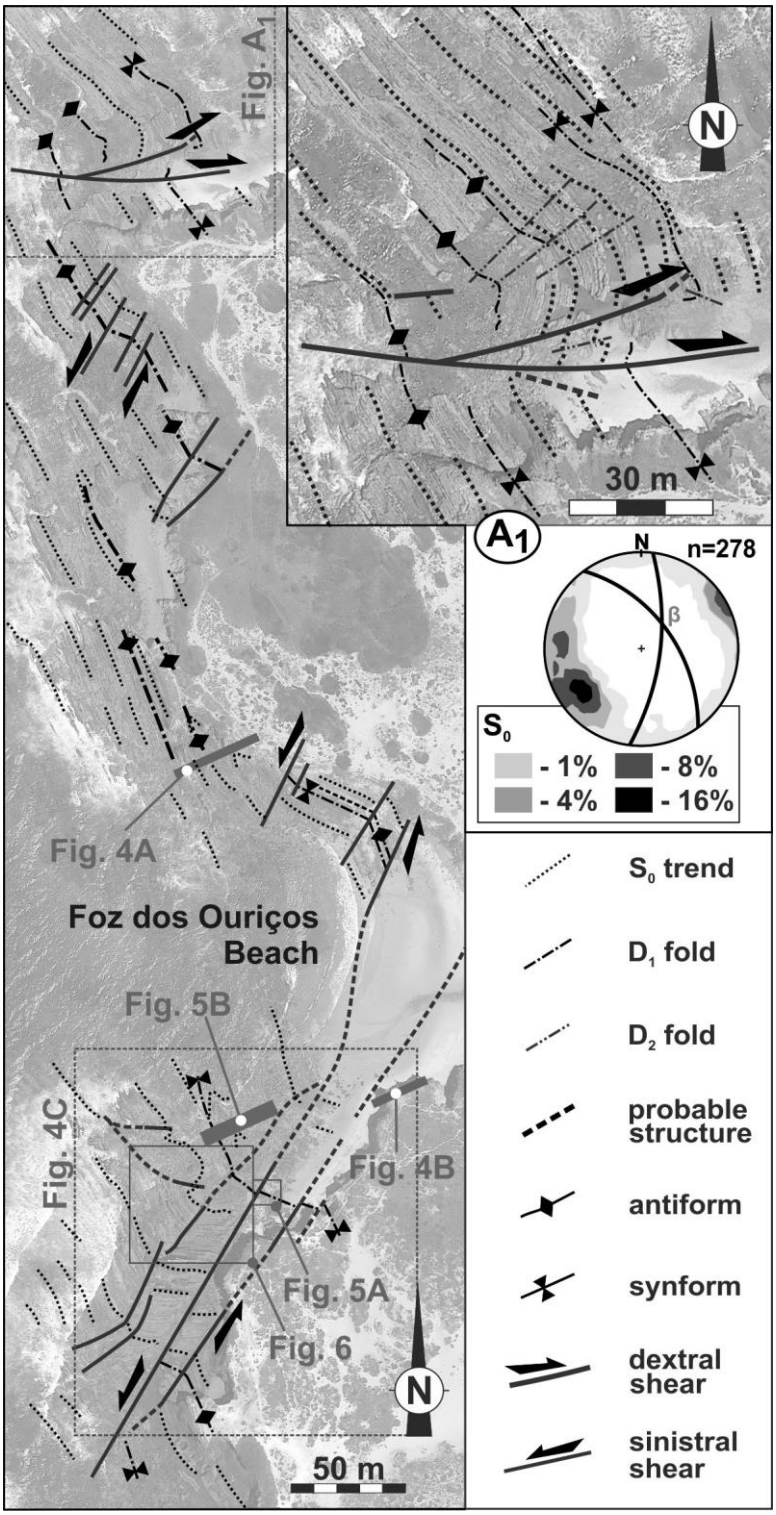

Figure 3 – General Variscan structural map for the Almograve-Foz dos Ouriços area. The inset (A_1) shows structural details of northern sector.

X.1.4.1.1. Structural Pattern of Almograve Sector

Concerning the Variscan major structure of Almograve, there is a strong contrast between the NNW-SSE bedding trend domains and the WNW-ESE to E-W ones (Fig. 4A$_2$).

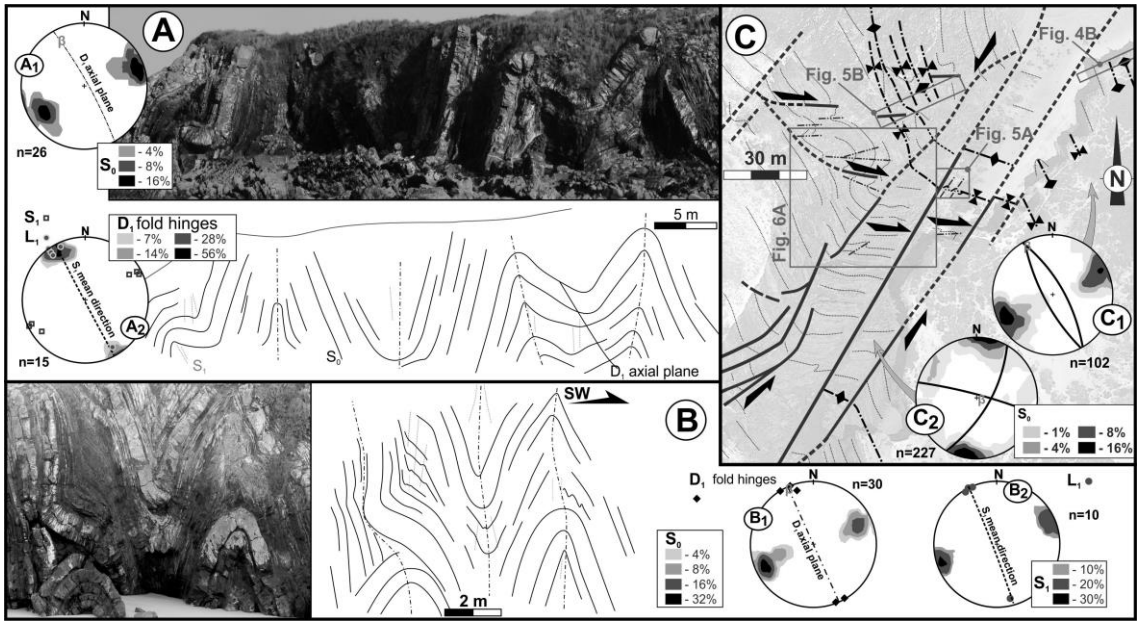

Figure 4 – Main geometry features of Variscan folds for the Almograve-Foz dos Ouriços beach NNW-SSE sectors (equal area lower hemisphere stereographic projections).

A – Fold array and geometrical data (A_1-bedding; A_2-D_1 fold hinges) in northern Foz dos Ouriços;

B – Fold array and geometrical data (B_1- D_1 fold hinges; B_2- L_1 intersection lineation) in southern Foz dos Ouriços;

C – Structural map of southern Foz dos Ouriços sectors with bedding stereographic analysis (symbols as in figure 3).

X.1.4.1.1.1. Variscan Folds

In the NNW-SSE segments (Figs. 4A; 4B), although the D_1 folds have sometimes complex shape profiles due to rheological contrasts of the turbiditic multilayer (Fig. 4B) and intense fluid migration (Marques *et al.*, 2010), they have a very regular, N20ºW - N30ºW trend (Figs. 4A$_1$, 4B$_1$ and 4C$_1$), which is also the direction of the locally developed axial planar S_1 cleavage (Fig. 4A$_2$ and 4B$_2$). When present, the L_1 intersection lineation (S_0^S_1) is subhorizontal or very low dipping to NNW (usually <10º), being subparallel to the fold hinges (Figs. 4A$_2$ and 4B$_2$). As the axial planes are subvertical, the folds in Foz dos Ouriços/Almograve have no clear vergence, although immediately SW of the studied domain the SW vergence is well expressed (Dias and Basile, 2013).

The Variscan folds in the WNW-ESE to E-W sectors have a much more complex geometry due to the pervasive superposition of a different folding event. The pattern of these post-D_1 folds are highly heterogeneous due to the coexistence of two completely different set of D_2 folds, which are easily distinguish by their symmetry in an orthorhombic (Fig. 5) and a monoclinic set (Fig. 6).

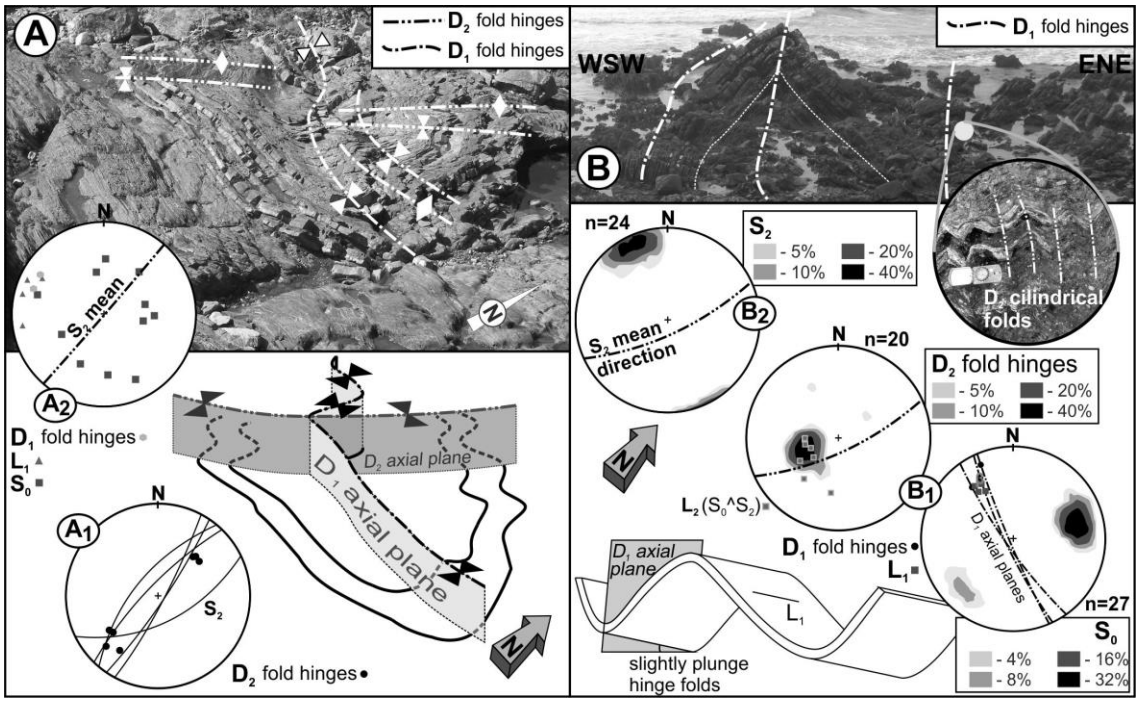

Figure 5 – NNE-SSW orthorhombic D_2 structures in the E-W Almograve sector (equal area lower hemisphere stereographic projections).

A – Wavy D_2 hinges in a D_1 syncline refolded by D_2 folds;

B – Moderate NNW dipping of D_1 folds overprinted by D_2 folding.

The orthorhombic D_2 folds (Fig. 5) have a NNE-SSW to NE-SW trend and variable axes, which were mostly controlled by the dip of the D_1 fold limbs (Figs. $5A_1$ and $5B_1$). The weak flattening related to these D_2 folding led to the development of an incipient S_2 crenulation cleavage, which is usually restricted to the more pelitic layers. When present, the S_2 cleavage (Figs. $5A_1$ and $5B_2$) is axial planar giving rise to a L_2 (S_0^S_2) intersection lineation parallel to D_2 hinges (Fig. $5A_2$ and $5B_2$).

As both the D_1 and the D_2 orthorhombic folds have subvertical axial planes and subperpendicular trends, a type 1 fold interference (Ramsay and Huber, 1987) was produced.

Although the D_2 orthorhombic folds are common in most of the WNW-ESE kinked domains, they are more frequent in the vicinity of the NNE-SSW faults that bound them. This

shows that such folds were developed due to the movement along these faults. The slight obliquity between the NE-SW folds and the N30ºE fault, is compatible with a sinistral kinematics along the NNE-SSW trend. Such conclusion is also supported by previous works in other sector of SW Portugal (Caroça and Dias, 2002), that described en-echelon NE-SW D_2 folds transected by an ENE-WSW S_2 cleavage, indicating a sinistral kinematics associated with NE-SW shear bands.

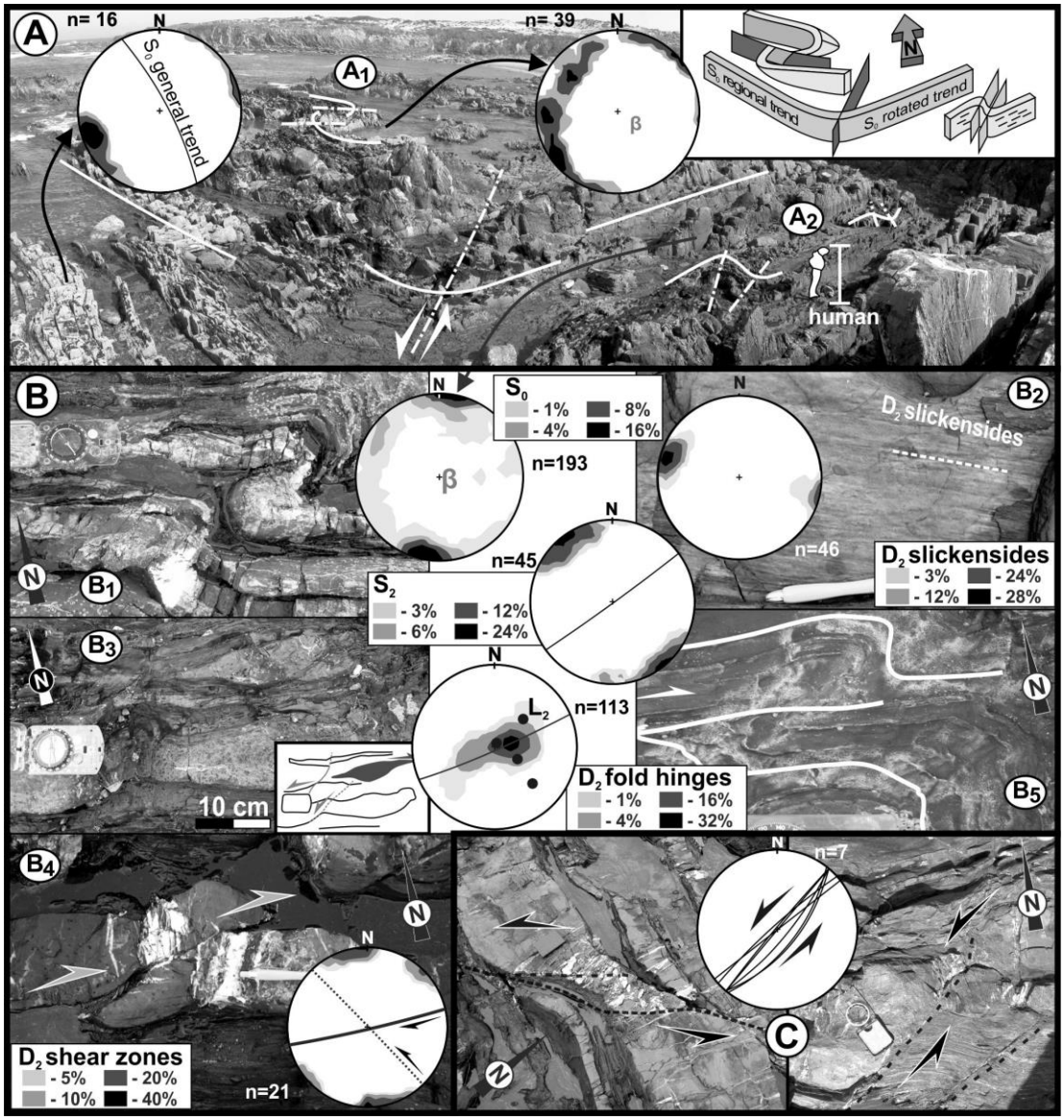

Figure 6 – Geometrical and kinematical features related with D_2 monoclinic structures in the E-W Almograve sector (equal area lower hemisphere stereographic projections).

A – Western boundary of the main Foz dos Ouriços kink-band (see Fig. 4A for location);

B – E-W D_2 dextral shear structures;

C – NNE-SSW D_2 sinistral shears.

Concerning the monoclinic D_2 folds set (Fig. 6) they are only found when the layers have strong dips and a trend close to E-W. They are also typical of places where the turbidites have a predominance of shales interbedded with centimetric to decimetric quartzwackes, often in the vicinity of metric quartzwacke layers not affected by such folding. These D_2 folds have subvertical axial planes slightly oblique to bedding trend, strongly plunging hinges and an eastern facing (Fig. $6B_1$). This geometry is compatible with a dextral shearing along the bedding. This is kinematically consistent with the subhorizontal slickensides in the bedding planes (Fig. $6B_2$), coupled with other sense of movement indicators, like sigma shape competent bodies (Fig. $6B_3$) or dextral faults (Fig. $6B_4$) often nucleating in the short limbs of these D_2 folds (Fig. $6B_5$).

Although both sets of D_2 folds are found in the WNW-ESE domain of the Almograve-Foz dos Ouriços kink-band, due to the different genetic mechanisms they were never observed in the same place. The absence of interference structures between both kinds of fold makes it difficult to determine their relative ages

X.1.4.1.1.2. Variscan Shear Zones

One of the most remarkable structures of Almograve are conjugated en echelon quartz veins related to the Variscan shear zones affecting quartz (Caroça and Dias, 2002; Marques *et al.*, 2010; Reber *et al.*, 2010; Zulauf *et al*, 2011; Dias and Basile, 2013). According to their temporal relation with the folds, they could be classified in two different sets: the early D_{1a} veins deformed by the regional folding (Fig. 7A), and the younger ones which have been superposed on the folds (Fig. 8A). Both families could also be distinguished by their geometries. While the acute angle between the older pre-folding conjugated shear zones is very small (23º to 31º; Fig. 7B), in the younger post folding veins such angle is always close to 60º (Fig. 8B). The unusual small angle between the pre-folding conjugated shear zones is not restricted to the Almograve sector and is the rule in the SW Iberia Variscides (Figs. 7C and 7D).

The temporal relation between the younger shear zones and both Variscan folding events (D_1 and D_2) is easy to establish. Indeed, the pattern of the stress field deduced by the conjugated shear zones in Almograve is consistently deflected by the D_2 major kink-folds (Fig. 8B): *i.e.* anticlockwise rotation in the E-W to WNW-ESE segments and clockwise in the NE-SW ones (Fig. 8C). The conclusion that these shear zones are pre-D_2 structures, is also consistent with the fact that, in each place where the stress field has been determined, the maximum principal compression (σ_1) stress is always orthogonal to the local fold trend (Fig. 8B). Thus the younger shear zones should be considered D_{1c} according to previous nomenclature (Fig. 2).

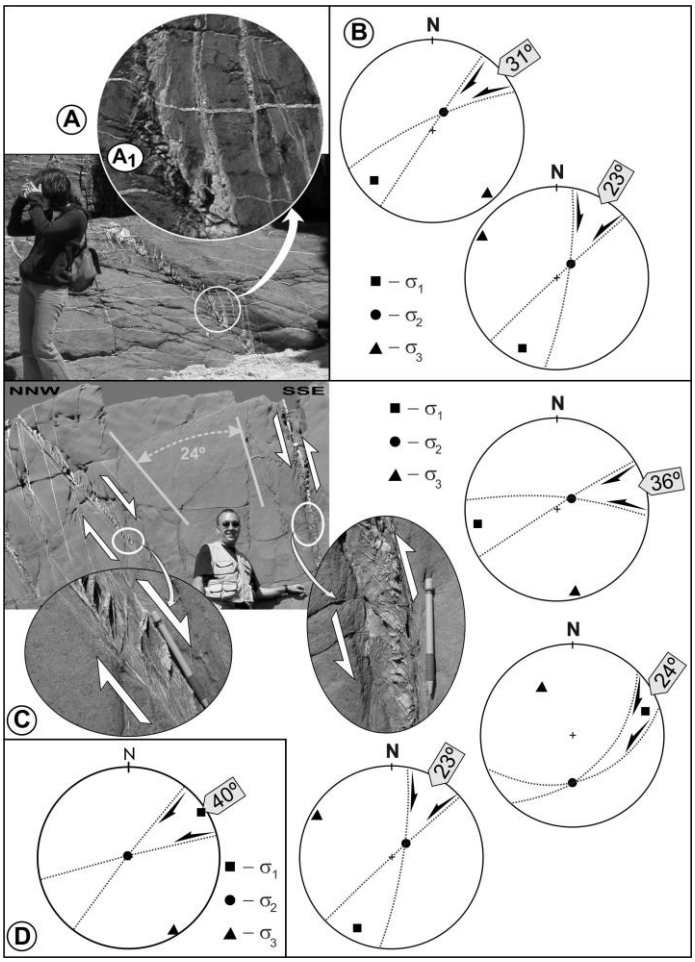

Figure 7 – Geometric and kinematic features of older conjugated Variscan shear zones in SW Iberia coast (equal area lower hemisphere stereographic projections):

A – En echelon quartz veins cut by outer arc fold extensional veins developed in Foz dos Ouriços beach folds (A_1);

B – Conjugated shear zones and related stress field for two situations in the southern domain of Almograve;

C – Conjugated shear zones and related stress field in the Arrifana sector;

D – Conjugated shear zones and related stress field for Cachado sector (north of Sagres).

Table 1 – Conjugated D_1 shear zones in SW Portugal.

sector	tectonic event	shear A		shear B		angle	σ_1	σ_2	σ_3
		attitude	kinem.	attitude	kinem.				
Almograve	**D_{1c}**	N40ºE,90	dextral	N80ºW,90	sinistral	60º	0º,N70ºE	90º	0º,N20ºW
Almograve	**D_{1c}**	N25ºE,80ºW	dextral	EW,70ºN	sinistral	63º	7º.S60ºW	70º,N8ºW	18º,S33ºE
Almograve	**D_{1c}**	N80ºE,75ºN	sinistral	N27ºE,75ºE	Dextral	58º	32º,S52ºW	58º,N54ºE	2º,N37ºW
Almograve	**D_{1a}**	N37ºE,90º	dextral	N68ºE,84ºS	sinistral	31º	20º,S50ºW	70º,N35ºE	5º,S42ºE
Almograve	**D_{1a}**	N56ºE,52ºS	normal	N62ºE,7º4S	reverse	23º	33º,N37ºE	56º,S51W	6º,S48ºE
Arrifana	**D_{1a}**	N68ºE,33ºS	---	N56ºE,68ºS	---	36º	14º,S78ºW	75º,N54ºE	5º,S13ºE
Arrifana	**D_{1a}**	N63ºE,53ºS	normal	N65ºE,77ºS	reverse	24º	20º,N71ºE	47º,S3ºW	37º,N35ºW
Arrifana	**D_{1a}**	N54ºE,83ºN	sinistral	N14ºE,80ºN	dextral	40º	14º,S28ºW	74º,N40ºE	4º,N62ºW
Cachado	**D_{1a}**	N77ºE,78ºN	sinistral	N40ºE,76ºN	dextral	36º	4º,N58ºE	86º,S80ºW	1º,S32ºE

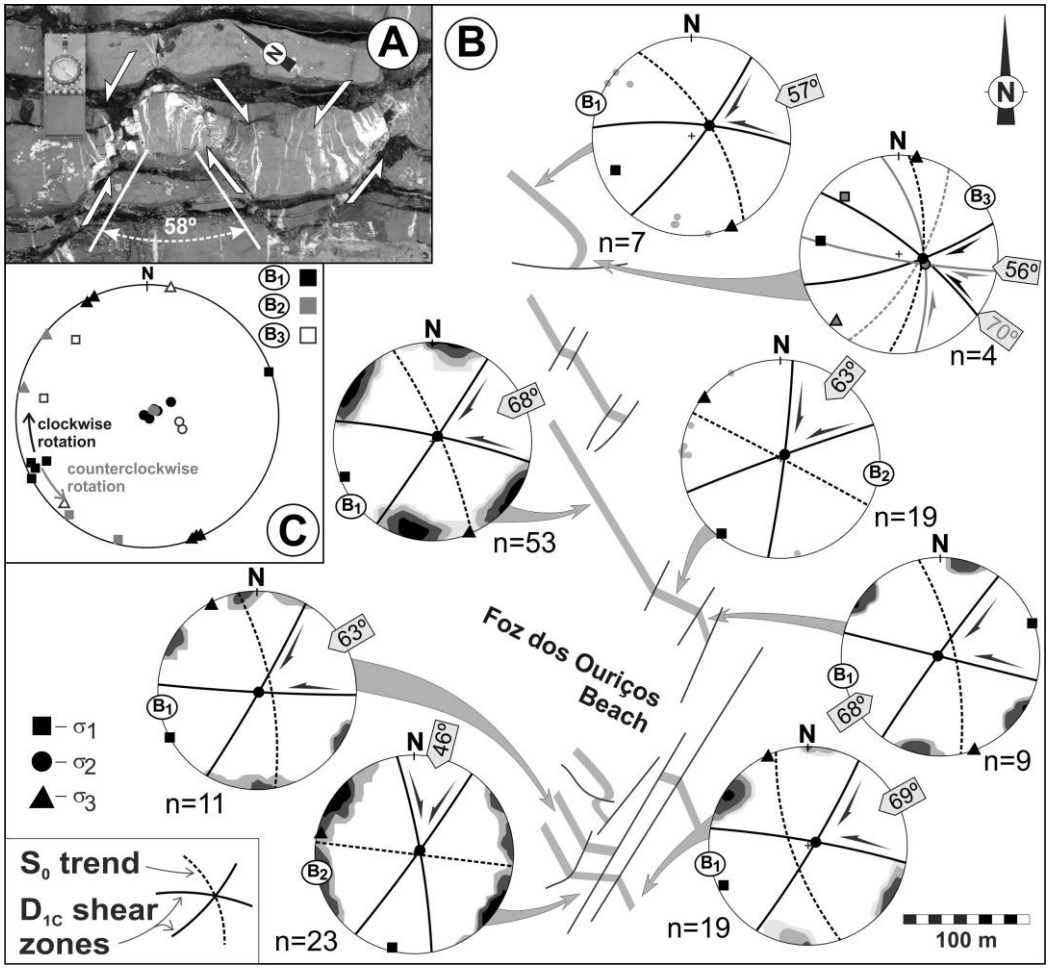

Figure 8 – Geometric and kinematic features of younger conjugated Variscan shear zones in Almograve (same area of figure 3):

A – Conjugated shear zones displacing strongly dipping layers of Almograve sector;

B – Conjugated shear zones and related stress field for several situations in the southern domain of Almograve (equal area lower hemisphere stereographic projections)

C – Compilation of Almograve stress field data.

The preservation of the stress field during the D_1 Variscan structures, shows a progressive and coaxial behaviour. However, if the orientation of the principal axes is preserved, the relative intensities between the main stresses change during the evolution of D_1 deformation (Table I). In the early D_{1a} stages, the acute angle is always below 40º (Fig. 7A), indicating the presence of hybrid fractures (Belayneh and Cosgrove, 2010) formed in a very low D_{1a} differential stress (σ_1-σ_3; Price and Cosgrove, 1990; Cosgrove, 2005). The acute angle is always very constant and close to the normal 60º for the late D_{1c} conjugate shears (Fig. 8B) expressing an higher differential stress (Belayneh and Cosgrove, 2010). Such a difference seems to indicate that during the D_{1c} the deformation occurred at a higher structural level than during

D_{1a}, which could result from the thickening of the turbiditic sequence due to the Variscan deformation. Indeed, the smaller D_{1a} acute angles could not be explained by the superposition of the flattening of younger D_{1b} or D_{1c} Variscan deformation events, because the similar orientation of their stress fields should have increase the initial angle whatever the limb in which they are found.

X.1.4.1.2. Variscan Kinematics of the NNE-SSW Fault Trend

The kinematics and age of the NNE-SSW major Variscan strike-slip faults in SW Portugal has been explained by two different opposite models:

- dextral and contemporaneous of the main D_1 regional folding event (Marques *et al.*, 2010; Fig. 9A);
- sinistral and younger than the main D_1 regional folding event (Caroça and Dias, 2002; Ribeiro *et al.*, 2007; Dias and Basile, 2013; Fig. 9B).

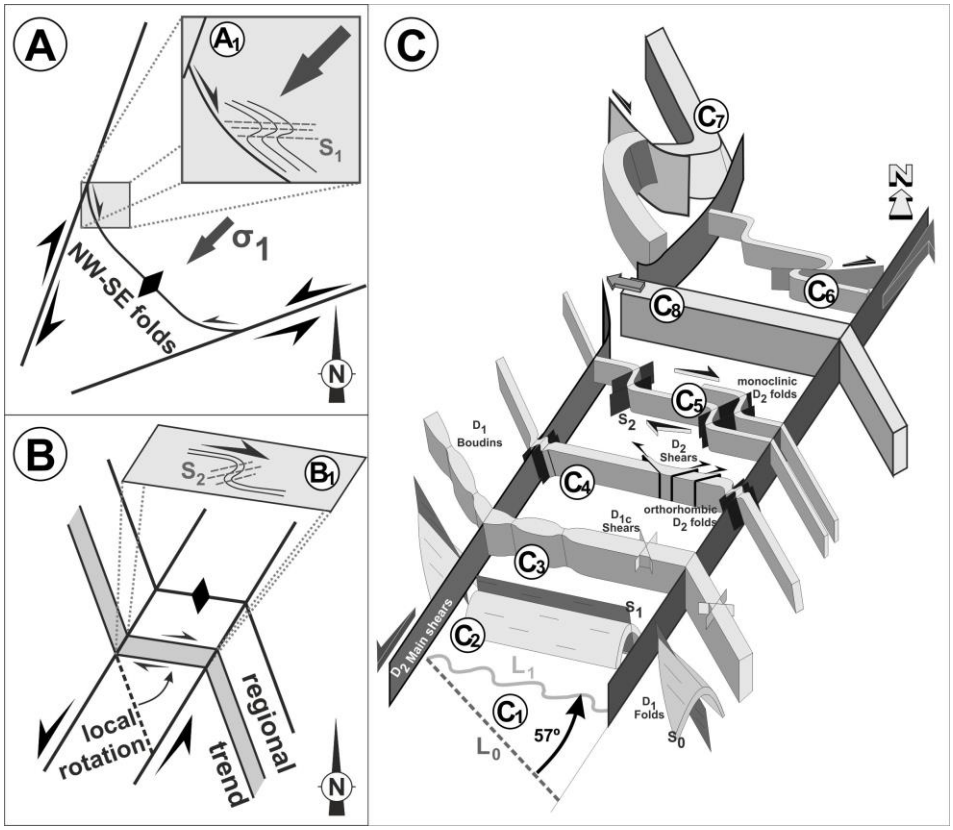

Figure 9 – Geometry and kinematics related to the NNE-SSW structures in SW Portugal.

A – The dextral model (adapted from Marques *et al.*, 2010);

B – The sinistral model (adapted from Caroça and Dias, 2002; Basile and Dias, 2013);

C – Main structural features related with the Foz dos Ouriços kink-band (see text for more details).

In the first model, the NNW-SSE structural trend is the result a local clockwise drag of the regional NW-SE structures due the dextral shearing along the major NNE-SSW wrench faults. This rotation, which was contemporaneous of the main D_1 folding event, gave rise to the E-W monoclinic folds, by a flattening mechanism induced by the interference between the regional compression and the dextral kinematics along the NNW-SSE layers (Fig. $9A_1$). Such dextral shearing was supported either by en-echelon quartz veins, or the deflection of sand dykes (figure 8 of Marques *et al.*, 2010). Concerning the quartz veins, care should be taken because described geometry, is also compatible with both dextral D_{1a} (Fig. 2A) and D_{1c} shears (Fig. 2D). Regarding the sand dykes, although they are usually considered to have initiated as orthogonal fractures to subhorizontal layers during diagenetic compaction (Cosgrove, 1997), field examples show that often they initiate oblique to the layering. This is clearly demonstrated by the coexistence in the same place of sand dykes with opposed deflections (Fig. 10). This strongly argued against the use of sand dykes as kinematic markers.

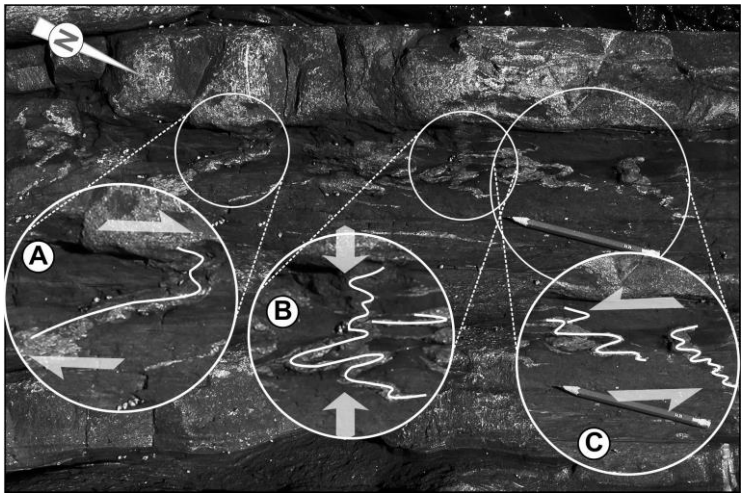

Figure 10 – Geometric complex behaviour of sedimentary dykes induced by diagenetic compaction in Arrifana port region.

A – Apparent dextral kinematics;

B – Orthogonal flattening;

C – Apparent sinistral kinematics.

It should be enhanced that, although the dextral kinematics along NNE-SSW faults could explain the ENE-WSW monoclinic folds (Fig. 6), it is unable to explain the frequent NE-SW orthorhombic folds (Fig. 5).

Moreover, the location of the younger D_2 structures only in the WNW-ESE kinked segment, shows that this orientation has only a local significance. Thus, the NNW-SSE general

trend in Almograve, where only the D_1 structures are found, must be considered the dominant regional trend, which have been anticlockwise deflected to WNW-ESE by the sinistral kink-band mechanism (Fig. 9B). Assuming such sinistral kinematics along the NNE-SSW faults, all the diversity of the structures found in Almograve could be explained (Fig. 9C). Indeed, the strong distortion related to the 57º rotation of the kink-band inner domain in relation with the outer NNW-SSE regional trend, superimposed on a highly anisotropic material, gave rise to the coexistence of different deformation mechanisms. Considering a constant width of the kink band (which is supported by the observation in the sectors near its extremities), and using the trends of the inner and outer domains, a 20% shortening should be expected during the rotation (Fig. $9C_1$). Thus, the simple and rigid rotation of previous D_1 structures (Figs. $9C_2$ and $9C_3$) cannot accommodate all the Late Variscan deformation inside the shear zone. As there is no evidence of considerable volume loss related with the D_2 phase (*e.g.* the intense quartz veining of Almograve is only related with the D_1 deformation), this orthogonal shortening must be compensated by subhorizontal and/or subvertical extension. The deformation induced by this shortening is heterogeneously distributed, being stronger in the vicinity of the kink band subvertical boundaries. The NNE-SSW to NE-SW D_2 folding with orthorhombic symmetry (Fig. 5), as well as conjugated shears displacing layer boundaries are due to such mechanism (Fig. $9C_4$). The lack of vergence of these folds, is explained by the subvertical geometry of the kink band limits which behaves as obstacles to the migration of the D_2 deformation.

The D_2 folds with subvertical hinges and a strong monoclinic symmetry highlight a strong dextral shearing subparallel to layers in the WNW-ESE inner domain (Figs. 6B and $9C_5$), this is an expected behaviour in some sinistral kink band (Ramsay and Huber, 1987; Twiss and Moores, 1992). Indeed, the progression of the sinistral rotation of the kink should be coupled with dextral shear strain on the rotating surfaces (Figs. $9C_5$ and $9C_6$).

The heterogeneities of the turbidite sequence could induce some irregularities in the structural pattern. The anomalous major fold (Figs. $6A_1$ and $9C_7$), although presenting a geometry similar to the D_2 monoclinic folds, is located outside the inner domain of the kink bands is attributed to the indentation of an anomalous metric thick quartzwacke package in adjacent pelitic zones (Fig. $9C_8$). Indeed, the shortening of such a competent package inside the kink band is difficult due to space considerations, which induce its indentation in the sectors adjacent to the kink band where incompetent shales are predominant. Such mechanism will produce, not only the folding/disruption of the boundaries of the kink band, but also anomalous folding in the domains adjacent to the indentor (Coke *et al.*, 2003).

It is worth to notice that in Northern domains of the studied Almograve Sector (Fig. 3), an important E-W dextral shear zone is found in places not related to sinistral kink bands. This shear zone generates a decametric drag fold, with NE-SW subvertical axial plane and steeply plunging hinge (Fig. $3A_1$), which rotate previous structures (Fig. 8B), showing that it is also related with the Late Variscan D_2 episode.

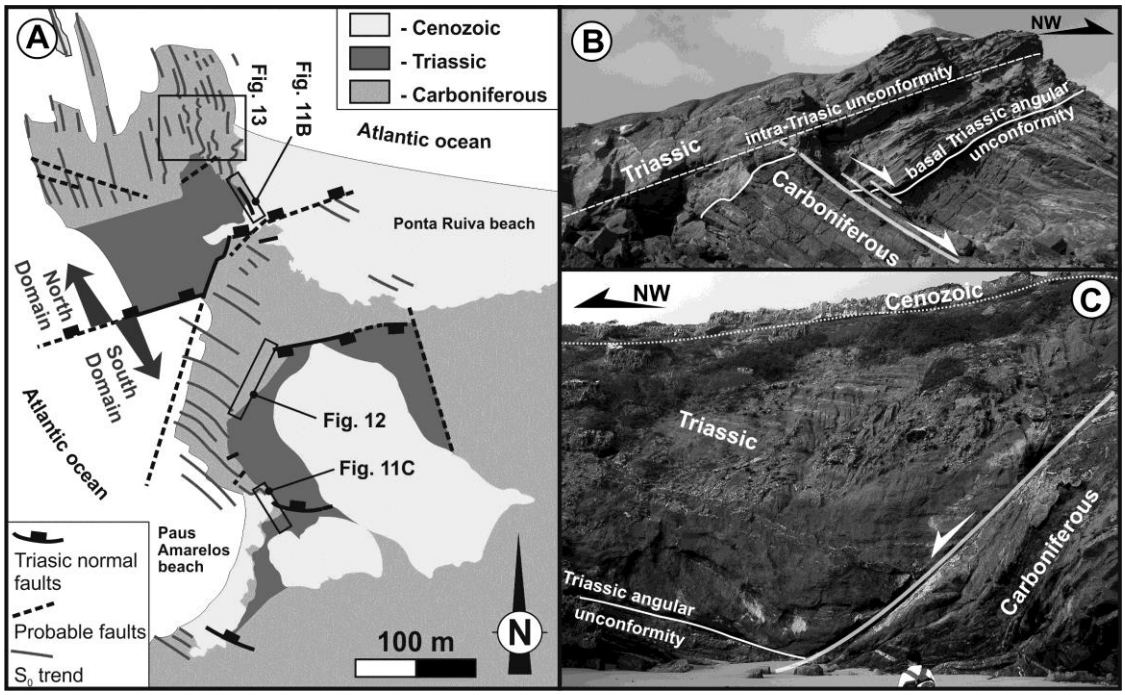

Figure 11 – General structural pattern of Ponte Ruiva area.

A – Structural map emphasizing main features related to D_2 deformation;

B – Triassic unconformity of the northern domain;

C – Triassic unconformity and extensional boundary fault of southern domain.

X.1.4.2. The Ponta Ruiva Sector

In Ponta Ruiva the angular unconformity between the weakly deformed Triassic sediments and the highly folded low metamorphosed Carboniferous units is exceptionally exposed (Fig. 11). As in Almograve, in Ponta Ruiva it is possible to observe adjacent sectors with contrasting Variscan trends (Fig. 11A): NNW-SSE and NW-SE. However, here the transition between both domains is harder to understand, not only due to a strong overprinting by the early episode related to the Atlantic opening, but also to the smaller extent of the outcrops in the wave cut platform. This younger extensional tectonic event gives rise to a complex set of small scale intracontinental basins filled by several syn-rift sedimentary units of Triassic

age (Dias and Ribeiro, 2002). The opening of these basins has been controlled by the reworking of previous Variscan anisotropies (Dias and Basile, 2013) with ENE-WSW to E-W trend.

X.1.4.2.1. Variscan Deformation Geometry in Ponta Ruiva Sector

The geometry of the Variscan deformation in the Carboniferous turbidites led to the individualization of two different domains in Ponta Ruiva (Fig. 11A):

- The southern domain is well expressed along the cliffs and the neighbouring wave cut platform. The main structure (Fig. 12) corresponds to a major NW-SE D_1 recumbent fold facing to SW with subhorizontal axial plane (Fig. 12A). The S_1 cleavage (Fig. 12B), which fans around the fold, is pervasive in the more pelitic layers. It has an axial plane attitude which is also confirmed by the parallelism between the subhorizontal L_1 (S_0^S_1) intersection lineation and the D_1 fold hinges (Fig. 12C). Locally, rare D_2 folds occur with subvertical axes (Fig. 11D), which are more frequent in the vicinity of the major extensional fault of the Paus Amarelos beach (Fig. 11C).

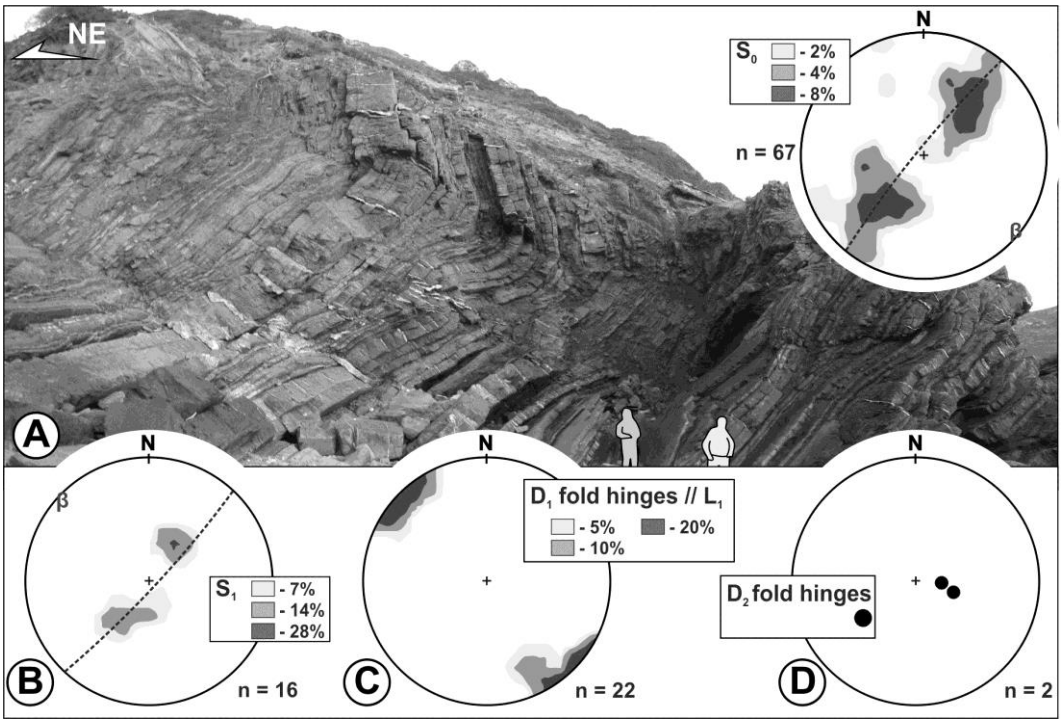

Figure 12 – Structural features in the southern domain of Ponta Ruiva (equal area lower hemisphere stereographic projections):

A – Main D_1 recumbent fold with bedding (S_0) geometry;

B – S_1 cleavage geometry;

C – Geometry of L_1 intersection lineation and D_1 hinges;

D – Geometry of D_2 hinges.

- The northern domain corresponds to the more external sector of the wave-cut platform, where the Variscan structure is a reverse limb of a major D_1 fold. The singularity of this domain in the regional context comes, not only from the NNW-SSE trend (Fig. 13A), but mostly from the dipping hinges of the minor D_1 folds (Fig. 13B and 13C). The present attitude of the fold axes (26º, N44ºW; Fig. 13C) would increase the plunge when the pre-Triassic position is restored by the removal of the Atlantic extensional deformation (37º, N52ºW; Fig. 13D). The plunging hinges of the D_1 mesoscopic folds show that the Variscan geometry of this domain is local and results from the distortion of the regional structure where the folds have always subhorizontal hinges, as observed in the southern domain (Ribeiro and Silva, 1983; Silva *et al.*, 1990; Dias and Basile, 2013).

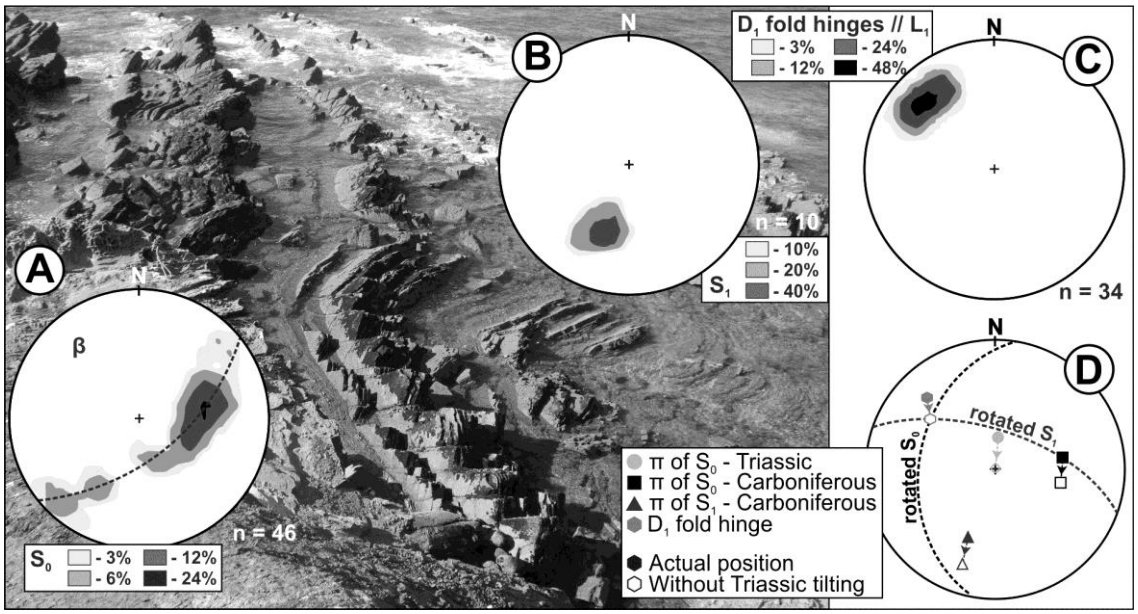

Figure 13 – Structural features in the northern domain of Ponta Ruiva (equal area lower hemisphere stereographic projections):

A – D_1 folds with bedding (S_0) geometry;

B – S_1 cleavage geometry;

C – Geometry of L_1 intersection lineation and D_1 hinges;

D – Rotation of D_1 structures associated with the removal of the Triassic deformation.

X.1.4.2.2. Structural Evolution of Ponta Ruiva Sector

The oldest structures of Ponta Ruiva are the NW-SE D_1 recumbent folds facing SW (Fig. 12A), which is the normal regional trend for the major Variscan folds in SW Portugal (Fig. 1; Ribeiro *et al.*, 1979). The dip of the axial surfaces is controlled by the proximity to major

thrusts (Ribeiro, 1983) and the sub-horizontal geometries observed in Ponta Ruiva results from the vicinity of D_1 major thrusts, which are frequent in SW Portugal (Fig. 1B; Dias and Basile, 2013).

The local rotation of the D_1 Variscan structures observed in the northern Ponta Ruiva domain (Fig. 11A) could not be explained by the Triassic extension and must have been induced by the Late Variscan deformation, which also produced the D_2 folds with subvertical axes (Fig. 12D). The ENE-WSW to E-W trend of the major boundary faults of Ponta Ruiva Triassic basins (Fig. 11A), suggests that such direction must have been dominant during Palaeozoic times. A dextral kinematics along the ENE-WSW boundary fault between the northern and southern domains (Fig. 14), similar to the Almograve Late Variscan behaviour (*i.e.* Fig. $3A_1$), with the expected coeval shortening in the rotated northern sector, explains, not only the more northerly trend but also the plunging hinges of the D_1 structures.

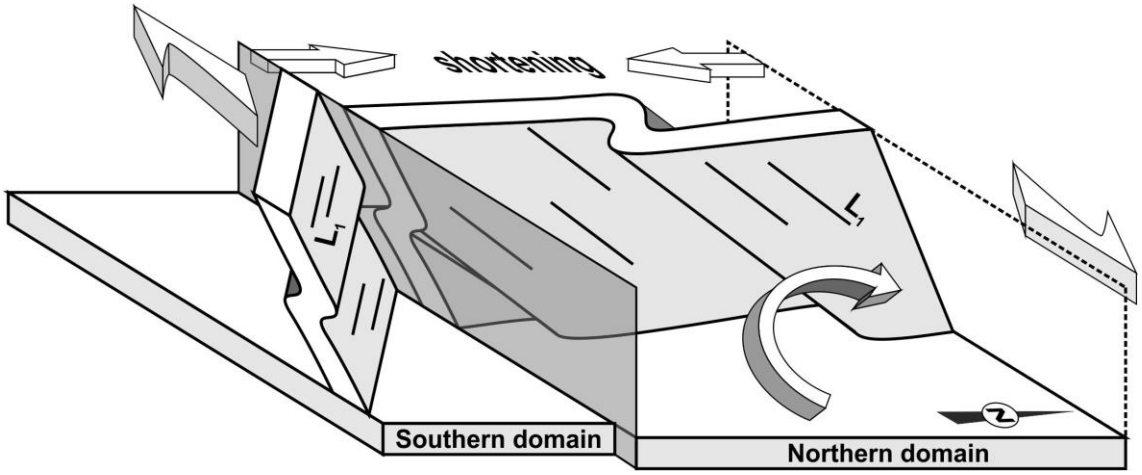

Figure 14 – Distortion of the D_1 structures by the Late Variscan ENE-WSW dextral shear.

The erosive processes, which became predominant after the last increments of the Variscan deformation, gave rise to a subhorizontal surface that is well preserved at the base of the Triassic sediments (Figs. 11B and 11C). The structural mapping of the Triassic-Carboniferous relations shows that the Ponta Ruiva basins opening was mostly controlled by E-W to ENE-WSW normal faults (Dias and Ribeiro, 2002), which locally reworked D_2 dextral strike-slip Late Variscan faults.

X.1.5. Geodynamical Implications

The new data from the SW Iberia help the understanding of Late Variscan geodynamical evolution. Indeed, they can be used to debate the kinematics of NNE-SSW Iberian wrench

faults, described in North of Portugal (*e.g.* Ribeiro, 1974; Ribeiro *et al.*, 1990; Lourenço *et al.*, 2002; Marques *et al.*, 2002; Ribeiro *et al.*, 2007), and also constrain their deformation ages.

X.1.5.1. The deformation ages of SW Iberia Structures

The older formation outcropping in the Almograve (Fig. 4) and Ponta Ruiva (Fig. 10) studied regions belongs to the Baixo Alentejo Flysch Group (Oliveira, 1990). Detailed paleontological studies (Pereira *et al.*, 2007; Jorge *et al.*, 2013; Oliveira *et al.*, 2013) show that this turbiditic formation is diachronous, ranging from Visean in the northern domains to Upper Moscovian in the southern tip. The paleocurrent indicators preserved in the turbidites (*e.g.* groove and flute casts) are often subperpendicular to the D_1 fold axes, which suggests that the sedimentation is coeval with the deformation (Oliveira, 1990; Dias and Basile, 2013). So, the main Variscan deformation of the Carboniferous turbidites (D_1) seems to be also diachronous, being older in the more internal NE domains (Ribeiro and Silva, 1983).

The age of the D_2 dextral shear zones could only be constrained in the Ponta Ruiva sector. The Carboniferous turbidites are here Upper Moscovian (Pereira *et al.*, 2007; Oliveira *et al.*, 2013) and have been strongly folded during D_1 (Figs. 12A and 13A; Caroça and Dias, 2001; Dias and Ribeiro, 2002; Dias and Basile, 2013). The younger sediments on top of the Carboniferous flysch of SW Portugal is at least Middle to Upper Triassic (Palain, 1976), but possibly could attain the Lower Triassic (Rocha, 1976). In Ponta Ruiva, these sediments have been shown to be syn-rift in relation to the early extensional stages of the Atlantic opening (Fig. 11B; Dias and Ribeiro, 2002). As the D_1 age should be close to the local Carboniferous sedimentation (*i.e.* Upper Moscovian) and the D_2 shear zones have been reactivated as normal faults during the Triassic extension, the age of D_2 phase is bracketed by these two events. This means that the D_2 in SW Portuguese coast must be considered a Late Variscan tectonic event, acting during Late Carboniferous and Permian times, as emphasized by Noronha *et al*. (1981) for the Central Iberian Zone in Northern Portugal.

X.1.5.2. The NNE-SSW Late Variscan Kinematics

As the Almograve structural data show (Fig. 9C), the NNE-SSW faults have a sinistral kinematics. This behaviour is pervasive along the SW Portuguese coast, where NNE-SSW to NE-SW hectometric faults and/or kink bands with metric to decametric sinistral displacements are common (Caroça and Dias, 2002; Dias and Basile, 2013). The strongly linear NNE-SSW trend of this coast, seems to indicate that it is controlled by a deep first order Late Variscan sinistral fault, whose superficial expression is the 2nd and 3rd order sinistral fault like structures found in

Almograve type faults (Fig. 15A; Caroça and Dias, 2002; Dias and Basile, 2013). The obliquity between both scales of faults indicates that the minor ones could be interpreted as *p*-type fractures inside a main shear zone (Fig. 15A). A comparison of the trend of the D_2 sinistral fractures of Almograve (NNE-SSW; Fig. 3) with the observed further to SW (NE-SW; Caroça and Dias, 2002) shows a slight rotation (Figs. $15A_1$ and $15A_2$). Such rotation accompanies the linear orientation of the Portuguese coast.

The existence of a probable major NNE-SSW Late Variscan left lateral fault in SW Iberia shows that the dominant trend of Late Variscan faults in northern Portugal (*e.g.* Vilariça and Régua-Chaves-Verin first order faults; Fig. 15B) are also found further south (Fig. 15A). As in SW Portugal the sinistral kinematics is clear (Figs. 4 and 9C), the same kinematics must be expected in the northern Portugal NNE-SSW faults. Nevertheless. although the sinistral kinematics during Late Variscan times is usually considered (Ribeiro, 1974; Ribeiro *et al.*, 1979; Iglesias and Ribeiro, 1981; Choukhroune and Iglésias, 1980; Pereira *et al.*, 1993; Ribeiro *et al.*, 2007; Moreira *et al.*, 2010; 2014; Dias *et al.*, 2013), an alternative proposal is that the sinistral sense was only an alpine reworking of a dextral NNE-SSW Late Variscan kinematics (Marques *et al.*, 2002; Lourenço *et al.*, 2002).

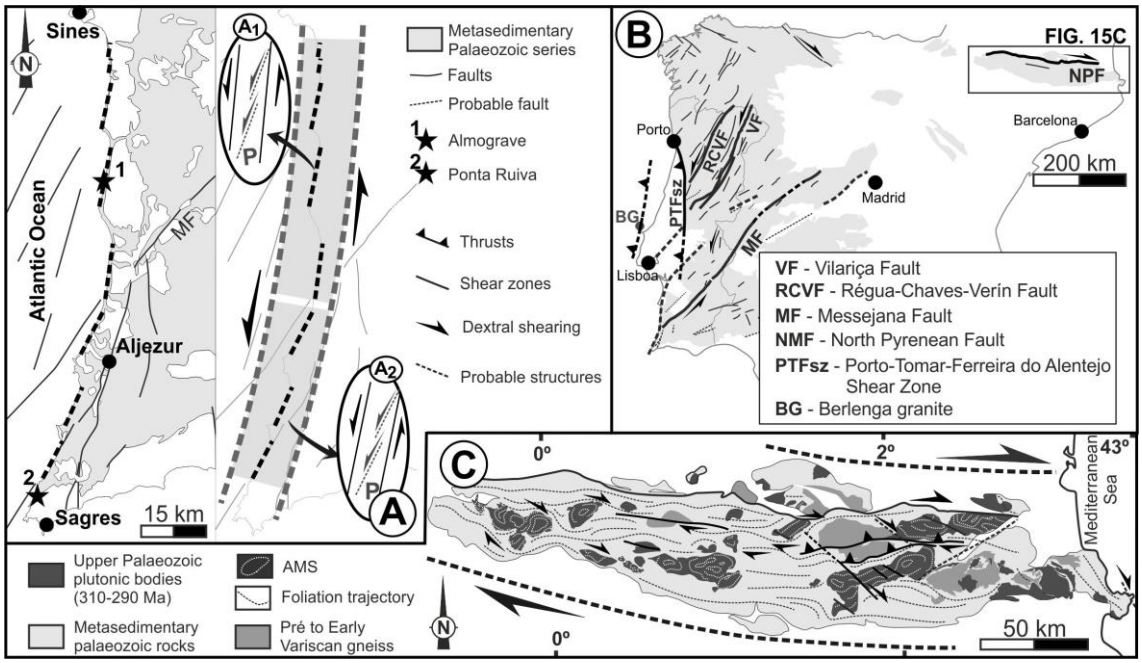

Figure 15 – Late Variscan structural behaviour in Iberia.

A – Interpretative fracture pattern along the SW Portuguese coast;

B – Main fracture pattern in Iberia;

C – Structural sketch of the Variscan Pyrenees (adapted from Zwart, 1986; Carreras, 2001; Denèle *et al.*, 2014).

The dextral interpretation was based essentially in the K-Ar 312 Ma age in muscovites concentrates from aplites and tourmaline-muscovite aggregates related to NE-SW segments in NNE-SSW faults in Northern Portugal (Marques *et al.*, 2002) and the geometrical / kinematical data from quartz veins, which are difficult to ascribe to the different tectonic events. Although these authors considered the obtained age a lower limit for the Late Variscan wrench faulting period, it could also be considered the upper limit for the D_3 Variscan regional event (Dallmeyer *et al.*, 1997). Thus, the proposed dextral movement along the NNE-SSW fault set should be considered as related, not with the Late Variscan kinematics (Marques *et al.*, 2002), but with the regional D_3 Variscan tectonic event as previously reported in several works (Ribeiro, 1974; Ribeiro *et al.*, 1979; Pereira *et al.*, 1993; Dias *et al.*, 2013; Noronha *et al.*, 2013). Therefore, the new data in SW Portuguese coast shows that the predominant movement in the NNE-SSW to NE-SW faults during Late Variscan times (i.e. Post-Moscovian - Pre-Triassic) was left-lateral, as proposed in early works (Ribeiro, 1974; Arthaud and Matte, 1975; 1977; Ribeiro *et al.*, 1979; Choukhroune and Iglésias, 1980; Iglesias and Ribeiro, 1981).

X.1.5.3. The E-W to ENE-WSW Dextral Kinematics

Even if the NNE-SSW fracture pattern has a pervasive development in Iberia (Fig. 15B), the SW Portuguese data show that the Late Variscan deformation cannot be understood without taking into account the E-W to ENE-WSW dextral shear zones. Indeed, although the sinistral NNE-SSW trend is usually more common, the dextral one sometimes becomes predominant.

The E-W to ESE-WNW structural trend is dominant in the axial zone of Pyrenees, in the Neoproterozoic and Palaeozoic rocks (Fig. 15C; *e.g.* Zwart, 1986; Castiñeiras *et al.*, 2008), where a polyphasic tectonotermal evolution with three Variscan deformation events is found (Carreras, 2001; Druguet, 2001). Such trend is usually correlated with the main Variscan tectonometamorphic event (local D_2) characterized by a dextral transpressional regime (Carreras and Druguet, 1994; Leblanc *et al.*, 1996; Druguet and Hutton, 1998; Gleizes *et al.*, 1998; Carreras, 2001; Druguet, 2001; Carreras *et al.*, 2004; Druguet *et al.*, 2014). The D_2 event is related with a progressive high temperature-low pressure metamorphic event (Druguet and Hutton, 1998; Druguet, 2001; Druguet *et al.*, 2014) associated with melt generation and the emplacement of an important set of plutonic bodies. Recent geochronological data constrain the age of emplacement of these syntectonic bodies between 310-290 Ma (*i.e.* Carboniferous-Permian transition; Denèle *et al.*, 2014; Druguet *et al.*, 2014; Pereira *et al.*, 2014), and consequently also constrain the age of the D_2 event. The anisotropy of magnetic susceptibility (AMS) shows clear evidence of dextral kinematics during the emplacement of these D_2

syntectonic plutonic bodies (Fig. 15C; Leblanc *et al.*, 1996; Gleizes *et al.*, 1997; 1998; Antolín-Tomás *et al.*, 2009; Denèle *et al.*, 2014). Gleizes *et al.* (1997; 1998) also remark the presence of continuous deformation from the magmatic state to the high-temperature solid state, which shows that dextral transpression remained active even after the emplacement. The previous data highlight an important Late Variscan WNW-ESE dextral tranpressive shear zone in the basement of the Axial Zone of the Pyrenees, which remained active from the Late Carboniferous until at least the Lower Permian.

Further South in Iberia, the predominance of E-W major right lateral shear zones during Late Variscan times could also be emphasized in the Azores-Gibraltar shear zone (Fig. 16; Ribeiro *et al.*, 2007; Dias *et al.*, 2016). However, these kinematics are poorly constrained due to their reworking as a plate boundary during the Pangaea breakup and the Alpine orogeny.

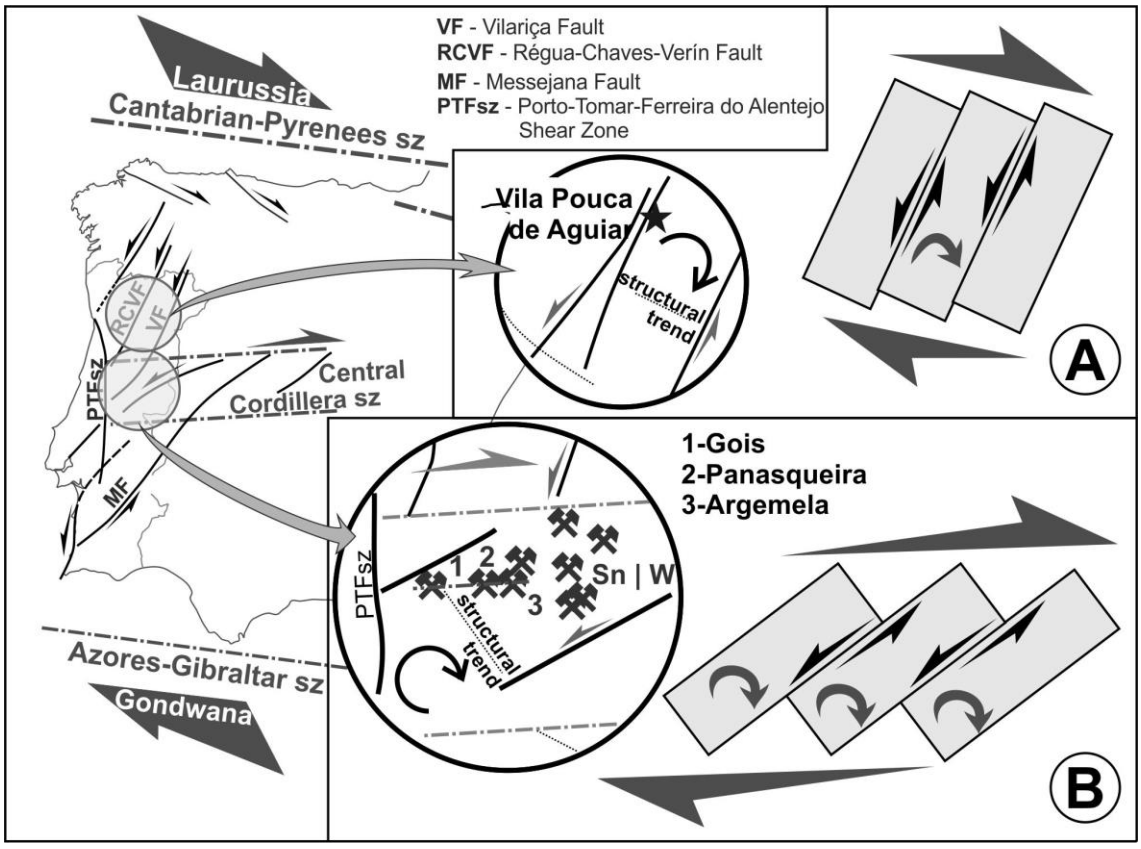

Figure 16 – Interpretative domino model for Iberian geodynamics during Late Variscan times (adapted from Ribeiro, 2002; ore occurrences adapted from Pereira *et al.*, 1993 and Noronha *et al.*, 2013).

A – NNE-SSW faults related to a low block rotation;

B – NE-SW faults related to a moderate/strong block rotation.

The major role that the E-W shear zones play in Iberia could be extended to the neighbouring regions. Indeed, they are also found, not only in southern France (Martínez-García, 1996), but also in the Moroccan Variscides (Piqué *et al.*, 1990; Houari and Hoepffner, 2003; Simancas *et al.*, 2005; Ribeiro, *et al.*, 2007). Although such major shear zones were already active since the main orogenic events, sometimes they are considered to be still active in Late Variscan times (Ribeiro *et al.,* 2007; Dias *et al.*, 2011).

X.1.5.4. An Unifying Approach

The absence of the dextral conjugated set (which in a brittle to brittle-ductile regime should be NNW-SSE; Ribeiro *et al.*, 1979), the relatively moderate offset comparing to the extension of the NNE-SSW major faults and the existence of N-S Late Variscan thrusts with an eastern displacement in the Berlengas archipelago (Fig. 15B), led Ribeiro (2002) to propose a domino model for the Late Variscan deformation (Fig. 16).

In this model, the dextral transpression induced by the Late Variscan oblique collision between Laurentia and Gondwana (Arthaud and Matte, 1975; 1977; Dias and Ribeiro, 1994; 1995; Ribeiro *et al.*, 1995: Shelley and Bossière, 2000; 2002; Ribeiro, 2002; Ribeiro *et al.*, 2007; Dias *et al.*, 2016) was mostly concentrated in the major E-W Iberian shear zones, located in Azores-Gibraltar and North Pyrenean shear zones. The domains between these shear zones where heterogeneously deformed. The important regional D_3 NNE-SSW tensile fractures in Central Iberian Zone (Ribeiro, 1974; Pereira *et al.*, 1993; Mateus, 1995) were rotated clockwise during the Late Variscan times. Such movement gave rise to a dextral domino due to the also clockwise rotation of the blocks bounded by the NNE-SSW faults, which thus will have a coeval sinistral kinematics (Figs. 16A and 16B; Ribeiro, 2002; Ribeiro *et al.*, 2007).

As expected, in a domino model, the amount of block rotation is strongly related with the intensity of distortion induced by the simple shear component. In Iberia, this is supported by the trend of the major sinistral Late Variscan faults (Dias *et al.*, 2013). The rotation from a NNE-SSW trend, either in northern (Fig. 16A; Régua-Chaves-Verin and Vilariça faults), or southern (Fig. 16; Messejana fault) sectors, to a NE-SW on Central Iberia (Fig. 16B), is explained by the lesser or stronger influence of the major ENE-WSW dextral Central Cordillera shear zone (Ribeiro, 2002). The same rotation is also observed using the main regional D_1 Variscan structures, whose general trend of folds have a WNW-ESE direction in northern Portugal (Fig. 16A), and a NW-SE in Central Portugal (Fig. 16B). The Central Cordillera shear zone is also enhanced by discrete E-W Late Variscan lineaments of Late Variscan mineralizations like the tin-tungsten-gold Góis-Panasqueira-Argemela band (Fig. 16B; Ribeiro and Pereira, 1982).

A similar deflection is found in the SW Portuguese coast (Caroça and Dias, 2002), with the main Late Variscan fractures rotating from NNE-SSW (Fig. 15A$_1$) towards NE-SW in the southern sectors (Fig. 15B). Such behaviour should be expected due to a closer proximity of the first order E-W dextral Azores-Gibraltar shear zone.

X.1.6. Conclusions

The principal outcomes of this study are concluded below:

i. The Variscan structures in the SW of South Portuguese Zone are the result of a long lasting diachronic process during the D_1 tectonic event, followed by D_2 deformation ascribed to the Late Variscan times;

ii. The NNE-SSW Late Variscan faults have a predominantly sinistral kinematics;

iii. The Late Variscan fault pattern in Iberia could be explained by a domino model controlled by E-W to ENE-WSW major dextral strike-slip shear zones, inducing the clockwise rotation of the blocks bounded by the NNE-SSW faults;

iv. This model could be considered an improvement of the dextral E-W mega-shear model of Arthaud and Matte (1975; 1977), between what they considered a northern American-European plate and a southern African one.

References

Abad, I., Nieto, F., Vellila, N., Simancas, J. (2004). Metamorfismo de la Zona Sudportuguesa. In: Vera J.A. (ed), Geologia de Espana. SGE-IGME, Madrid, 209-211.

Antolín-Tomás, B., Román-Berdiel, T., Casas-Sainz, A., Gil-Peña, I., Oliva, B., Soto, R. (2009). Structural and magnetic fabric study of the Marimanha granite (Axial Zone of the Pyrenees). Int. J. Earth Sci. (Geol Rundsch), 98, 427–441. DOI 10.1007/s00531-007-0248-1

Arthaud, F., Matte, Ph. (1975). Les decrochements tardi-hercyniens du sud-ouest de l'Europe, geometrie et essai de reconstitution des conditions de la deformation. Tectonophysics, 25, 139-171. doi:10.1016/0040-1951(75)90014-1

Arthaud, F., Matte, Ph. (1977). Late Paleozoic strike-slip faulting in southern Europe and northern Africa: result of a righ-lateral shear zone between the Appalachians and the Urals. Geol. Soc. Am. Bull., 88, 1305-1320. doi: 10.1130/0016-7606(1977)88<1305:LPSFIS>2.0.CO

Belayneh, M., Cosgrove, J. (2010). Hybrid veins from the southern margin of the Bristol Channel Basin, UK. J. Struct. Geology, 32, 192–201. doi:10.1016/j.jsg.2009.11.010

Bradley, D.C., Kidd, W.S.F. (1991). Flexural extension of the upper continental crust in collisional foredeeps, Geological Society of America Bulletin, 103(11), 1416-1438. DOI: 10.1130/0016-7606(1991)103<1416:FEOTUC>2.3.CO;2

Caroça, C., Dias, R. (2001). Estrutura Varisca na região de Sagres; um exemplo de deformação progressiva. Comun. Inst. Geol. Min. Portugal, 88, 1-16.

Caroça, C., Dias, R. (2002). Deformação transcorrente nos sectores externos da zona Sul Portuguesa; os últimos incrementos da tectónica Varisca, Comun. Inst. Geol. Min. Portugal, 89, 115-126.

Carreras, J. (2001). Zooming on Northern Cap the Creus Shear Zones, J. Struct. Geol., 23, 1457-1486. DOI: 10.1016/S0191-8141(01)00011-6

Carreras, J., Druguet, E. (1994). Structural zonation as a result of inhomogeneous non-coaxial deformation and its control on syntectonic intrusions: an example from the Cap de Creus area (eastern-Pyrenees). J. Struct. Geol., 16, 1525–1534. DOI:10.1016/0191-8141(94)90030-2

Carreras, J., Druguet, E., Griera, A., Soldevila, J. (2004). Strain and deformation history in a syntectonic pluton. The case of the Roses granodiorite (Cap de Creus, Eastern Pyrenees). In: Alsop, G.I., Holdsworth, R., McCaffrey, K., Hand, W. (Eds.), Flow Processes in Faults and Shear Zones. Geol. Soc. London, 224, 307–19. DOI:10.1144/GSL.SP.2004.224.01.19

Carvalho, D., Goinhas, J., Oliveira, V., Ribeiro, A. (1971). Observações sobre a geologia do Sul de Portugal e consequências metalogenéticas. Est. Notas e Trab. Serv. Fom. Min., 20, 153-199.

Castiñeiras, P., Navidad, M., Liesa, M., Carreras, J., Casas, J.M. (2008). U–Pb zircon ages (SHRIMP) for Cadomian and Early Ordovician magmatism in the Eastern Pyrenees: new insights into the pre-Variscan evolution of the northern Gondwana margin. Tectonophysics, 461, 228–39. DOI: 10.1016/j.tecto.2008.04.005

Choukhroune, P., Iglésias, M. (1980). Zonas de cisalla dúctil en el NW de la Peninsula Ibérica. Cuad. Lab. Xeol. Laxe, 1, 163-164.

Coke, C., Dias, R., Ribeiro, A. (2003). Rheologically induced structural anomalies in transpressive regimes, J. Struct. Geol., 25(3), 409-420. DOI: 10.1016/S0191-8141(02)00043-3

Cosgrove, J. (1997). Hydraulic fractures and their implications regarding the state of stress in a sedimentary sequence during burial. In: Sengupta, S. (Ed.), Evolution of Geological Structures in Micro- to Macro-scales, Chapman & Hall, 11-25. DOI: 10.1007/978-94-011-5870-1_2

Cosgrove, J. (2005). Tectonics: Fractures (Including joints). In: Selley, R.C., Cocks, L.R.M., Plimer, I.R. (Eds.), Encyclopedia of Geology, Elsevier Academic Press, 352-361.

Dallmeyer, D., Martínez Catalán, J., Arenas, R., Gil Ibarguchi, J., Gutiérrez Alonzo, G., Farias, P., Bastida, F., Aller, J. (1997). Diachronous Variscan tectonothermal activity in the NW Iberian Massif: Evidence from 40Ar/39Ar dating of regional fabrics. Tectonophysics, 277, 307-337. DOI:10.1016/S0040-1951(97)00035-8

Denèle, Y., Laumonier, B., Paquette, J., Olivier, Ph., Gleizes, G., Barbey, P. (2014). Timing of granite emplacement, crustal flow and gneiss dome formation in the Variscan segment of the Pyrenees. In: Schulmann, K., Martínez Catalán, J.R., Lardeaux, J.M., Janousek, V., Oggiano, G. (Eds.) The Variscan Orogeny: Extent, Timescale and the Formation of the European Crust. Geol. Soc. London, 405, 265-287. DOI:10.1144/SP405.5

Dias, R., Ribeiro, A. (1994). Constriction in a transpressive regime: an example in the Ibero-Armoricain Arc. J. Struct. Geol., 16(11), 1543-1554. DOI:10.1016/0191-8141(94)90032-9

Dias, R., Ribeiro, A. (1995). The Ibero-Armorican arc: a collisional effect against an irregular continent? Tectonophysics, 246(1-3), 113-128. DOI:10.1016/0040-1951(94)00253-6

Dias, R., Ribeiro, C. (2002). O Triásico da Ponta Ruiva (Sagres); um fenómeno localizado na Bacia Mesozóica Algarvia. Comun. Inst. Geol. Min Portugal, 89, 39-46.

Dias, R., Basile, C. (2013). Estrutura dos sectores externos da Zona Sul Portuguesa; implicações geodinâmicas. In: Dias, R., Araújo, A., Terrinha, P., Kullberg, J.C. (Eds.), Geologia de Portugal, vol. 1, Escolar Editora, 787-807.

Dias, R., Hadani, M., Leal Machado, I., Adnane, N., Hendaq, Y., Madih, K., Matos, C. (2011). Variscan structural evolution of the western High Atlas and the Haouz plain (Morocco). Journal of African Earth Science, 61, 331-342. DOI:10.1016/j.jafrearsci.2011.07.002

Dias, R., Ribeiro, A., Coke, C., Pereira, E., Rodrigues, J., Castro, P., Moreira, N., Rebelo, J. (2013). Evolução estrutural dos sectores setentrionais do autóctone da Zona Centro-Ibérica. In: Dias, R., Araújo, A., Terrinha, P., Kullberg, J.C. (Eds.), Geologia de Portugal, vol. 1, Escolar Editora, 73-147.

Dias, R., Ribeiro, A., Romão, J., Coke, C., Moreira, N. (2016). A Review of the Arcuate Structures in the Iberian Variscides; Constraints and Genetical Models. Tectonophysics, 681, 170-194. DOI: 10.1016/j.tecto.2016.04.011

Druguet, E. (2001). Development of high thermal gradients by coeval transpression and magmatism during the Variscan orogeny: insights from the Cap de Creus (Eastern Pyrenees). Tectonophysics, 332, 275–293. DOI:10.1016/S0040-1951(00)00261-4

Druguet, E., Hutton, D. (1998). Syntectonic anatexis and magmatism in a mid-crustal transpressional shear zone: an example from the Hercynian rocks of the eastern Pyrenees. J. Struct. Geol., 20, 905–916. DOI: 10.1016/S0191-8141(98)00017-0

Druguet, E., Castro, A., Chichorro, M., Pereira, M., Fernández, C. (2014). Zircon geochronology of intrusive rocks from Cap de Creus, Eastern Pyrenees Geol. Mag., 151(6), 1095–1114. DOI: 10.1017/S0016756814000041

Gleizes, G., Leblanc, D., Bouchez, J. (1997). Variscan granites of the Pyrenees revisited: their role as syntectonic markers of the orogen. Terra Nova, 9, 38–41. DOI: 10.1046/j.1365-3121.1997.d01-9.x

Gleizes, G., Leblanc, D., Santana, V., Olivier, Ph., Bouchez, J. (1998). Sigmoidal structures featuring dextral shear during emplacement of the Hercynian granite complex of Cauterets-Panticosa (Pyrenees). J. Struct. Geol., 20(9-10), 1229-1245. DOI:10.1016/S0191-8141(98)00060-1

Houari, M., Hoepffner, C. (2003). Late Carboniferous dextral wrench-dominated transpression along the North African craton margin (Eastern High-Atlas, Morocco). Journal of African Earth Science, 37, 11-24. DOI:10.1016/S0899-5362(03)00085-X

Iglesias, M., Ribeiro, A. (1981). Zones de cisaillement ductile dans l'arc ibéro-armoricain. Comun. Serv. Geol.Portugal, 67, 85-87.

Jorge, R., Fernandes, P., Rodrigues, B., Pereira, Z., Oliveira, J.T. (2013). Geochemistry and provenance of the Carboniferous Baixo Alentejo Flysch Group, South Portuguese Zone. Sedimentary Geology, 284/285, 133-148. DOI: 10.1016/j.sedgeo.2012.12.005.

Leblanc, D., Gleizes, G., Roux, L., Bouchez, J. (1996). Variscan dextral transpression in the French Pyrenees: new data from the Pic des Trois-Seigneurs granodiorite and its country rocks. Tectonophysics, 261, 331–45. DOI:10.1016/0040-1951(95)00174-3

Lourenço, J., Mateus, A., Coke, C., Ribeiro, A. (2002). A zona de falha Penacova-Régua-Verín na região de Telões (Vila Pouca de Aguiar); alguns elementos determinantes da sua evolução em tempos tardivariscos. Comum. Inst. Geol. Mineiro, 89, 105-122.

Marques, F., Mateus, A., Tassinari, C. (2002). The Late-Variscan fault network in central-northern Portugal (NW Iberia): a re-evaluation. Tectonophysics, 359, 255-270. DOI:10.1016/S0040-1951(02)00514-0

Marques, F., Burg, J., Lechmann, S., Schmalholz, S. (2010). Fluid-assisted particulate flow of turbidites at very low temperature: A key to tight folding in a submarine Variscan foreland basin of SW Europe. Tectonics, 29. DOI:10.1029/2008TC002439

Martínez-García, E. (1996). Correlation of Hercynian units of the Iberin massif and southeartern France. Geogaceta, 20(2), 468-471.

Martínez Catalán, J. (2011). Are the oroclines of the Variscan belt related to late Variscan strike-slip tectonics? Terra Nova, 23, 241–247.

Mateus, A. (1995). Evolução tectono-térmica e potencial metalogenético do troço transmontano da Zona da Falha Manteigas-Vilariça-Bragança, Ph. D. Thesis, Lisbon University, 1189 p.

Moreira, N., Dias, R., Coke, C., Búrcio ,M. (2010). Partição da deformação Varisca nos sectores de Peso da Régua e Vila Nova de Foz Côa (Autóctone da Zona Centro Ibérica); Implicações Geodinâmicas. Comunicações Geológicas, 97, 147-162.

Moreira, N., Araújo, A., Pedro, J.C., Dias, R. (2014). Geodynamic evolution of Ossa-Morena Zone in SW Iberian context during the Variscan Cycle. Comunicações Geológicas, 101(I), 275-278.

Munhá, J. (1983). Hercynian magmatism in the Iberian Pyrite Belt. In: Lemos de Sousa, M., Oliveira, J.T. (Eds.), The Carboniferous of Portugal. Memórias dos Serviços Geológicos de Portugal, 29, 39-81.

Nance, R., Gutiérrez-Alonso, G., Keppie, J., Linnemann, U., Murphy, J., Quesada, C., Strachan, R., Woodcock, N. (2012). A brief history of the Rheic Ocean. Geoscience Frontiers, 3(2), 125-135. DOI:10.1016/j.gsf.2011.11.008

Noronha, F., Ramos, J.M.F., Rebelo, J.A., Ribeiro, A., Ribeiro, M.L. (1981). Essai de corrélation des phases de déformation hercynienne dans le nord-ouest Peninsulaire. *Leidse Geol. Medlingen,* 52 (1), 87-91.

Noronha, F., Ribeiro, M.A., Almeida, A., Dória, A., Guedes, A., Lima A., Martins, H.C., Sant'Óvaia, H., Nogueira, P., Martins, T., Ramos, R., Vieira, R. (2013). Jazigos Filonianos Hidrotermais e Aplitopegmatíticos espacialmente associados a Granitos (Norte de Portugal). In: Dias, R., Araújo, A., Terrinha, P., Kullberg, J.C. (Eds.), Geologia de Portugal, vol. 1, Escolar Editora, 403-438.

Oliveira, J.T. (1984). Carta geológica de Portugal. Escala 1/200.000. Notícia explicativa da Folha 7 (coord), Serviços Geológicos de Portugal.

Oliveira, J.T. (1990). South Portuguese Zone, stratigraphy and synsedimentary tectonism. In: Dallmeyer, R., Martinez Garcia, E. (Eds.), Pre-Mesozoic Geology of Iberia, Springer-Verlag, 334-347.

Oliveira, J.T., Relvas, J., Pereira, Z., Matos, J., Rosa, C., Rosa, D., Munhá, J.., Fernandes, P., Jorge, R.C.G.S., Pinto, A. (2013). Geologia da Zona Sul Portuguesa, com ênfase na estratigrafia, vulcanologia física, geoquímica e mineralizações da Faixa Piritosa. In: Dias, R., Araújo, A., Terrinha, P., Kullberg, J.C. (Eds.), Geologia de Portugal, vol. 1, Escolar Editora, 673-765.

Palain, C. (1976). Une série détritique terrigéne. Les Grés de Silves. Trias et Lias inférieur du Portugal, Mem. 25 (Nova Série) Serviços Geológicos de Portugal.

Pereira, E., Ribeiro, A., Meireles, C. (1993). Cisalhamentos hercínicos e controlo das mineralizações de Sn-W, Au e U na Zona Centro-Ibérica em Portugal. Cuaderno Lab. Xeolóxico de Laxe, 18, 89-119.

Pereira, M.F., Castro, A., Chichorro, M., Fernández, C., Díaz-Alvarado, J., Martí, M., Rodríguez, C., (2014). Chronological link between deep-seated processes in magma chambers and eruptions: Permo-Carboniferous magmatism in the core of Pangaea (Southern Pyrenees). Gondwana Research, 25, 290–308. DOI: 10.1016/j.gr.2013.03.009

Pereira, Z., Matos, J., Fernandes, P., Oliveira, J.T. (2007). Devonian and Carboniferous palynostratigraphy of the South Portuguese Zone, Portugal - An overview. Comunicações Geológicas, 94, 53-79.

Piqué, A., Cornee, J., Muller, J., Roussel, J. (1990). The Moroccan Hercynides. In: Dallmeyer R. D., Lécorché, J. P. (Eds.), "The West African orogens and circum Atlantic correlatives", Springer Verlag, 229-262.

Price, N., Cosgrove, J. (1990). Analysis of geological structures. Cambridge University Press.

Ramsay, J., Huber, M. (1987). The techniques of modern structural geology. Vol.1. Folds and fractures. Academic Press, Inc., London.

Reber, J., Schmalholz, S., Burg, J. (2010). Stress orientation and fracturing during three-dimensional buckling: numerical simulation and application to chocolate-tablet structures in folded turbidites, SW Portugal. Tectonophysics, 493, 187-195. DOI:10.1016/j.tecto.2010.07.016

Ribeiro, A. (1974). Contribuition à l'étude tectonique de Trás-os-Montes. Mem. Serv. Geol. Portugal, 24.

Ribeiro, A. (1983). Structure of the Carrapateira nappe in Bordeira area. south-west Portugal. In: Lemos de Sousa, M. J., Oliveira, J.T. (Eds.), The Carboniferous of Portugal, Mem. Serv. Geol. Portugal, 29, 91-97.

Ribeiro, A. (2002). Soft Plate Tectonics. Springer-Verlag, Berlin, 324 p.

Ribeiro, A., Pereira, E. (1982). Controles paleogeográficos, petrológicos e estruturais na génese dos jazigos portugueses de estanho e volfrámio. Geonovas, 1(3), 23-31.

Ribeiro, A., Silva, J. (1983). Structure of the South Portuguese Zone. In: Lemos de Sousa, M. J., Oliveira, J.T. (Eds.), The Carboniferous of Portugal, Mem. Serv. Geol. Portugal, 29, 83-89.

Ribeiro, A., Antunes, M.T., Ferreira, M.P., Rocha, R.B., Soares, A.F., Zbyszewski, G., Moitinho de Almeida, F., Carvalho, D., Monteiro, J.H. (1979). Introduction à la Géologie Générale du Portugal. Serviços Geológicos de Portugal.

Ribeiro, A., Oliveira, J.T., Silva, J. (1983). La estrutura de la Zona Sur Portuguesa. In: Comba, J.A. (Ed.), Geologia de España, Inst. Geol. Min. Esp. Madrid, 1, 504-511.

Ribeiro A, Pereira E, Dias R (1990) Structure of Centro-Iberian allochthon in northern Portugal. In: Dallmeyer, R., Martinez Garcia, E., (Eds.), Pre-Mesozoic Geology of Iberia, Springer-Verlag, 220-236.

Ribeiro, A., Dias, R., Silva, J. (1995). Genesis of the Ibero-Armorican Arc. Geodinamica Acta, 8(2), 173-184. DOI:10.1080/09853111.1995.11417255

Ribeiro, A., Munhá, J., Dias, R., Mateus, A., Pereira, E., Ribeiro, L., Fonseca, P., Araújo, A., Oliveira, T., Romão, J., Chaminé, H., Coke, C., Pedro, J. (2007). Geodynamic evolution of SW Europe Variscides. Tectonics, 26, 1-24. DOI: 10.1029/2006TC002058

Rocha, R. (1976). Estudo estratigráfico e paleontológico do Jurássico do Algarve ocidental. Ciências Terra, 2.

Schermerhorn, L. (1971). An outline stratigraphy of the Iberian Pyrite Belt. Bol. Geol. Min. España, 82(3-4), 239-268.

Scisciani, V., Calamita, F., Tavarnelli, E., Rusciadelli, G., Ori, G.G., Paltrinieri, W. (2001). Foreland-dipping normal faults in the inner edges of syn-orogenic basins: A case from the Central Apennines, Italy. Tectonophysics, 330, 211-224. DOI: 10.1016/S0040-1951(00)00229-8

Shelley, D., Bossière, G. (2000). A new model for the Hercynian Orogen of Gondwanan France and Iberia. J. Struct. Geol., 22, 757-776. DOI:10.1016/S0191-8141(00)00007-9

Shelley, D., Bossière, G. (2002). Megadisplacements and the Hercynian orogen of Gondwanan France and Iberia. In: Martínez Catalán, J., Hatcher, Jr.R.., Arenas, R., Díaz García, F. (Eds), Variscan-Appalachian dynamics: The building of the late Paleozoic basement: Boulder, Colorado. Geological Society of America, Special Paper, 364, 209–222. DOI: 10.1130/0-8137-2364-7.209

Silva, J. (1989). Estrutura de uma geotransversal da faixa piritosa: zona do vale do Guadiana. PhD Thesis, Lisbon University.

Silva, J., Oliveira, J., Ribeiro, A. (1990). South Portuguese Zone, structural outline. In: Dallmeyer, R., Martinez Garcia, E. (Eds.), Pre-Mesozoic Geology of Iberia, Springer-Verlag, 348-362.

Simancas, J., Tahiri, A., Azor, A., Lodeiro, F., Poyatos, D., Hadi, H. (2005). The tectonic frame of the Variscan-Alleghanian orogen in southern Europe and Northern Africa. Tectonophysics, 398, 181-198. DOI:10.1016/j.tecto.2005.02.006

Twiss, R., Moores, E. (1992). Structural Geology. W. H. Freeman and Company.

Zulauf, G., Gutiérrez-Alonso, G., Krausc, R., Petschick, R., Potel, S. (2011). Formation of chocolate-tablet boudins in a foreland fold and thrust belt: A case study from the external Variscides (Almograve, Portugal). J. Struct. Geol., 33, 1639-1649. DOI:10.1016/j.jsg.2011.08.009

Zwart, H. (1986). The Variscan Geology of Pyrenees, Tectonophyics, 129, 9-27. DOI:10.1016/0040-1951(86)90243-X